6-10-2014 12:00 AM

Characterization of the anti-apoptotic function of the lysine demethylase plant homeodomain finger protein 8 (PHF8)

Kimberly Muranko, *The University of Western Ontario*

Supervisor: Dr. Shawn Li, *The University of Western Ontario*

A thesis submitted in partial fulfillment of the requirements for the Master of Science degree in Biochemistry

CHARACTERIZATION OF THE ANTI-APOPTOTIC FUNCTION OF THE LYSINE DEMETHYLASE PLANT HOMEODOMAIN FINGER PROTEIN 8 (PHF8)

(Thesis format: Monograph)

by

Kimberly Muranko

Graduate Program in Biochemistry

A thesis submitted in partial fulfillment
of the requirements for the degree of
Master of Science

The School of Graduate and Postdoctoral Studies
The University of Western Ontario
London, Ontario, Canada

Abstract

Apoptosis is an essential process in development and tissue maintenance. The tumor suppressor protein p53 initiates apoptosis through transactivation of pro-apoptotic genes when cellular stress is detected. This study identifies a regulatory role for the lysine demethylase, PHF8, in the p53-mediated apoptosis pathway. We initially suspected PHF8 of demethylating the adaptor protein Numb, however found this to be untrue. PHF8 has been found to have oncogenic properties including an anti-apoptotic effect, however how PHF8 negatively affects apoptosis has not been previously investigated. We found PHF8 inhibits translation of the pro-apoptotic genes *TP53, BAX* and *CASP3*. Chromatin immunoprecipitation revealed PHF8 binding to the *TP53* and *CASP3* gene promoters. H3K27 methylation at these promoters was significantly decreased with doxorubicin treatment in the presence of PHF8, and significantly increased when PHF8 was knocked down. Since methylated H3K27 is a repressive mark, we suspect other transcription factors or histone modifying proteins to be involved.

Keywords

Apoptosis, Numb, PHF8, p53, Caspase3, demethylation, epigenetics, demethylase, chemotherapy, cell death.

Acknowledgments

I would like to thank Dr. Shawn Li for his guidance and allowing me carry out my graduate research in his lab. I would also like to thank my other committee members Dr. Chris Brandl and Dr. Cheryl Seguin for their helpful advice throughout my studies. I would also like to extend thanks to Dr. Fred Dick for providing me with cell lines (although not used in this study) and his advice. Special thanks extended to Dr. Kristin Chadwick for training me in Flow cytometry analysis.

There are many members of the Li lab, former and present, whom have helped me throughout my time in the Li lab. I greatly appreciate the friendship and support of Ran Wei, Dr. Shelley Sandiford and Dr. Gurpreet Dhami. I appreciate the technical support I received from Courtney Voss, Chengjun Li and Dr. Huadong Liu. I am very thankful for all the help I have received from Dr. Kyle Biggar; helping me with statistics and proofreading and editing my thesis.

My parents have been a significant support throughout my entire university career. I am very grateful for all they do for me. Finally, I would like to extend my deepest gratitude to my boyfriend Eric Sylvain. He has been a tremendous emotional support for me during my graduate degree. I fear I would not have been successful without his never ending love and motivation.

Table of Contents

List of Tables

List of Figures

List of Appendices

List of Abbreviations

Apaf-1	Apoptosis-protease activating factor 1
ATM	Ataxia-telangiectasia, mutated
ATP	Adenosine tri-phosphate
ATR	ATM and Rad3-related
BAD	B-cell lymphoma (Bcl)-2-associated death promoter
BAX	Bcl-2-associated x protein
Bcl-2	B-cell lymphoma 2
Caspase3	Cysteine-dependent aspartate-directed protease 3
Caspase9	Cysteine-dependent aspartate-directed protease 9
CDK1	Cyclin dependent kinase 1
ChIP	Chromatin immunoprecipitation
Chk1	Checkpoint kinase 1
Chk2	Checkpoint kinase 2
CASP3	Caspase3 gene
DBD	DNA binding domain
DMEM	Dulbecco's modified eagle's medium
DNA	Deoxyribonucleic acid
DOX	Doxorubicin
DPF	Aspartic acid-proline-phenylalanine

E2F1	E2F transcription factor 1
EH	Esp15 homology
ESCC	Esophageal squamous cell carcinoma
FAS	First apoptosis signal
FBS	Fetal bovine serum
GAPDH	Glyceraldehyde 3-phosphate dehydrogenase
H3	Histone H3
H4	Histone H4
HRP	Horseradish peroxidase
IP	Immunoprecipitation
JmjC	Jumonji C
JHDM	JmjC demethylase
K	Lysine
KDM	Lysine demethylase
KMT	Lysine methyltransferase
LSD1	Lysine specific demethylase 1
MDM2	Mouse double minute 2 homologue
mRNA	Messenger ribonucleic acid
NCBI	National Center for Biotechnology Information
NLS	Nuclear localization sequence/signal

Noxa	Latin for damage; also known as Phorbol-12-myristate-13-acetate-induced protein 1
NPF	Asparagine-proline-phenylalanine
p21	Protein 21 kDa
p53	Protein 53 kDa
PBS	Phosphate buffered saline
PCR	Polymerase chain reaction
PEI	Polyethylenimine
PHD	Plant homology domain
PHF8	Plant homeodomain finger protein 8
PI	Propidium iodide
PML	Promyelocytic leukemia
PMSF	phenylmethanesulfonyl fluoride
PolII	RNA polymerase II
PRR	Proline rich region
PRRi	PRR region with sequence insertion
PRRo	PRR region without sequence insertion
PTB	Phosphotyrosine binding
PTBi	PTB domain with sequence insertion
PTBo	PTB domain without sequence insertion
PTM	Post-translational modification

PUMA	p53 up-regulated modulator of apoptosis
PVDF	Polyvinylidene fluoride
qRT-PCR	Quantitative real-time polymerase chain reaction
RARα	Retinoic acid receptor alpha
RNA	Ribonucleic acid
Rpl13	60S ribosomal protein L13
TBST	Tris-buffered saline with tween
TNFR	Tumor necrosis factor receptor
TP53	Tumor protein p53 gene
SDS-PAGE	Sodium dodecyl sulfate- polyacrylamide gel electrophoresis
Ser	Serine
SET1	**S**u(var)3-9, **E**nhancer of Zeste, **T**rithorax 1
SET7/9	**S**u(var)3-9, **E**nhancer of Zeste, **T**rithorax 7/9
SET8	**S**u(var)3-9, **E**nhancer of Zeste, **T**rithorax 8
SV40	Simian virus 40
WB	Western blot
XLMR	X-linked mental retardation

Chapter 1

1 Introduction

Post-translational modifications (PTM) play an important role in protein regulation. There are many different types of PTMs including phosphorylation, acetylation, glycosylation, as well as methylation an area of PMT research that is under rapid growth. The first histone methyltransferase, Su(var)3-9 human 1 (SUV39H1) was discovered in 2000 (Rea *et al*., 2000). Methylation of histone tail residues has become well characterized and is known to affect the regulation of gene expression by recruiting or inhibiting other regulatory proteins (Zhang and Reinberg, 2001). Methyltransferases have since been found to target either lysine or arginine histone tail residues (Zhang and Reinberg, 2001). Interestingly, until the discovery of the first demethylase, lysine specific demethylase 1 (LSD1), which removes methyl groups from histone H3 lysine 4, methylation was thought to be a static modification (Shi *et al*., 2004). Another relatively recent discovery was the methylation of non-histone proteins. The p53 protein was the first non-histone protein discovered to undergo post-translational methylation (Chuikov *et al*., 2004) and since this discovery, many non-histone methylation targets have been identified (Huang and Berger, 2008). Lysine methylation can act as either a positive or negative regulatory signal, existing in three states, mono-, di- and tri-methylation (Margueron *et al*., 2005). Each different methylation state on the same amino acid can elicit a different regulatory effect on the protein. Methylation has been found to play a role in regulating nearly all cellular processes, including cell proliferation, differentiation and apoptosis to name a few (Shi and Whetstine, 2006; Meek and Anderson, 2009). This study will focus on the role of methylation in regulating apoptosis.

1.1 Apoptosis

Cells death is an important process for the development and survival of multicellular organisms. During development, cells are required to undergo apoptosis in order for organ development and appendages to form (Horvitz, 1999; Renehan *et al*., 2001). By having a controlled manner of disposing of unwanted cells, an immune response is

avoided (Renehan *et al*., 2001). Apoptosis is also critical to the general maintenance and protection of tissues. Controlled cell death is the organism's way of disposing cells that are no longer necessary or could become harmful and cause damage to the tissue (Renehan *et al*., 2001). For example when a cell acquires DNA damage that cannot be repaired, it is in the body's best interest to prevent this cell from replicating and remove it, avoiding daughter cells which may have harmful mutations. Improper repair of DNA damage by avoiding cell cycle arrest and failure of cells to undergo apoptosis are hallmarks of cancer (Hanahan and Weinberg, 2000).

Apoptosis signalling occurs in response to a variety of different pathological and physiological stimuli. Depending on which stimuli the cell is responding to, different pathways and proteins will become active. The two main types of apoptotic pathways are the extrinsic pathway and the intrinsic pathway (Elmore, 2007). The extrinsic pathway involves an external ligand binding to a trans-membrane death receptor [i.e. Tumor necrosis factor receptor (TNFR), first apoptosis signal (FAS) receptor, etc.] (Locksley *et al*., 2001), whereas the intrinsic pathway results from an internal signal such as oncogene expression, excess DNA damage, hypoxia, toxins, or radiation (Elmore, 2007).

1.2 Tumor suppressor protein p53

1.2.1 Discovery of p53

The p53 protein was originally identified in 1979 as a protein found to bind the large 'T' antigen in simian virus 40 (SV40) transformed cells (Kress *et al*., 1979; Lane and Crawford, 1979; Linzer and Levine, 1979). It was identified as a 53kDa protein and therefore was named p53, representing a protein with a molecular weight of 53 kDa (Crawford, 1983). Since its discovery, p53 has been identified as a tumour suppressor protein in response to its cellular protective functions. In this regard, the p53 protein protects the cell in a number of ways such as regulating cell cycle check points (Kuerbitz *et al*., 1992), DNA damage response and repair, cell stress response and apoptosis induction (Meek, 2009), as well as regulating the inhibition of angiogenesis (Tokino and Nakamura, 2000). These functions are regulated by p53 through its role as a transcription factor. Therefore, p53 exerts its protective effects on cells by up-regulating the

transcription of genes required for these processes (Riley *et al*., 2008). The p53-induced gene expression includes the genes of proteins required for apoptosis such as pro-apoptotic proteins B-cell lymphoma (Bcl)-2-associated x protein (BAX) (Miyashita *et al*., 1994), Phorbol-12-myristate-13-acetate-induced protein 1 (NOXA) (Oda *et al*., 2000) and p53 up-regulated modulator of apoptosis (PUMA) (Nakano and Vousden, 2001), as well as genes required for the cell cycle arrest and DNA damage response (Levine, 1997) such as the cell cycle cyclin dependent kinase (cdk) inhibitor p21 (El-Deiry, 1993). Although p53 functions largely as a transcription factor, there is also evidence that p53 directly regulates proteins during apoptosis such as BAX (Chipuk *et al*., 2004).

Critically, the p53 protein has been reported to be deregulated in at least 50% of cancers (Soussi and Berude, 2001). In these cases, the p53 gene itself is either mutated or there are mutations in one of the many proteins that regulate p53 function or stability. For this reason, p53 has been studied intensely over the years in hopes to treat these cancers by reversing the negative effect on p53 function. However, our understanding of p53 function and its regulation remains incomplete and should remain an important focus of study for the development of new therapies for personalized cancer treatment.

1.2.2 p53 mediated apoptosis

The p53 mediated apoptosis pathway is induced by a number of signals (Elmore, 2007). These include aberrant oncogene expression, excessive DNA damage and hypoxia (Elmore, 2007; Gotz and Montenarh, 1995). In this manner, p53 is able to activate both the intrinsic and extrinsic apoptosis pathways. The extrinsic apoptosis pathway can be activated by p53 transactivation of the FAS receptor. Whereas, the p53 mediated intrinsic apoptosis pathway signalling (Figure 1.1) involves activation of pro-apoptotic Bcl-2 family proteins such as BAX, facilitating the release of cytochrome C from the mitochondria. Since p53 plays such an important protective role, it is constantly being synthesized in cells, but is also being constantly degraded, stabilized only when required by the cell. This constant synthesis of p53 allows for a quick response to cellular stress.

Ataxia-telangiectasia, mutated (ATM) and ATM and Rad3-related (ATR) are two kinases which sense genotoxic stress (Yang *et al*., 2004). When DNA damage is present, these

two kinases become activated. They can either directly activate p53 by phosphorylating p53 themselves or indirectly by activating other proteins which can then act on p53 (Yang *et al*., 2004). Both ATM and ATR have been found to phosphorylate a number of residues on p53 including serine 15 (Ser15) which leads to p53 activation (Canman *et al*., 1998; Tibbetts *et al*., 1999). ATM has been found to phosphorylate Ser46 of p53 which has been suggested to lead to p53's transactivation of proapoptotic genes (Saito *et al*., 2002).

Activation of p53 allows it to activate the expression of proapoptotic genes PUMA, BAX and Phorbol-12-myristate-13-acetate-induced protein 1 (NOXA) (Nakano and Vousden, 2001; Miyashita *et al*., 1994; Oda *et al*., 2000). These proteins inhibit Bcl-2, an anti-apoptotic protein, while stimulating the release of cytochrome C from the mitochondria. BAX binds to anti-apoptotic Bcl-2 family members when the cell is not undergoing apoptosis, which inhibits its apoptotic function (Oltvai *et al*., 1993). PUMA is able to inhibit the anti-apoptotic Bcl-2 proteins, releasing BAX and allowing it to form dimers with other pro-apoptotic Bcl-2 family members (Kuwana *et al*., 2005; Follis *et al*., 2013). These BAX dimers can them permeabilize the outer mitochondrial membrane causing the release of cytochrome C (Gross *et al*., 1999). Cytochrome C is then able to bind to and activate apoptosis-protease activating factor 1 (Apaf-1) hepta-oligomer along with adenosine tri-phosphate (ATP), forming the apoptosome (Garrido *et al*., 2006). The apoptosome is a complex which cleaves pro- cysteine-dependent aspartate-directed protease-9 (pro-Caspase9) to activate it and causes subsequent cleavage and activation of downstream caspases (Acehan *et al*., 2002). This leads to fragmentation of the nuclear envelope, degradation of nuclear and cytoskeletal proteins, as well as the degradation of chromosomal DNA (Elmore, 2007). The apoptotic cells and fragments are engulfed by phagocytes through the recognition of a phosphatidylserine on the cell surface (Wu *et al*., 2006). This phosphatidylserine is normally found within the membrane bi-layer, however when cells undergo apoptosis it is flipped out to be recognized on the surface of the cell (Fadok *et al*., 1998).

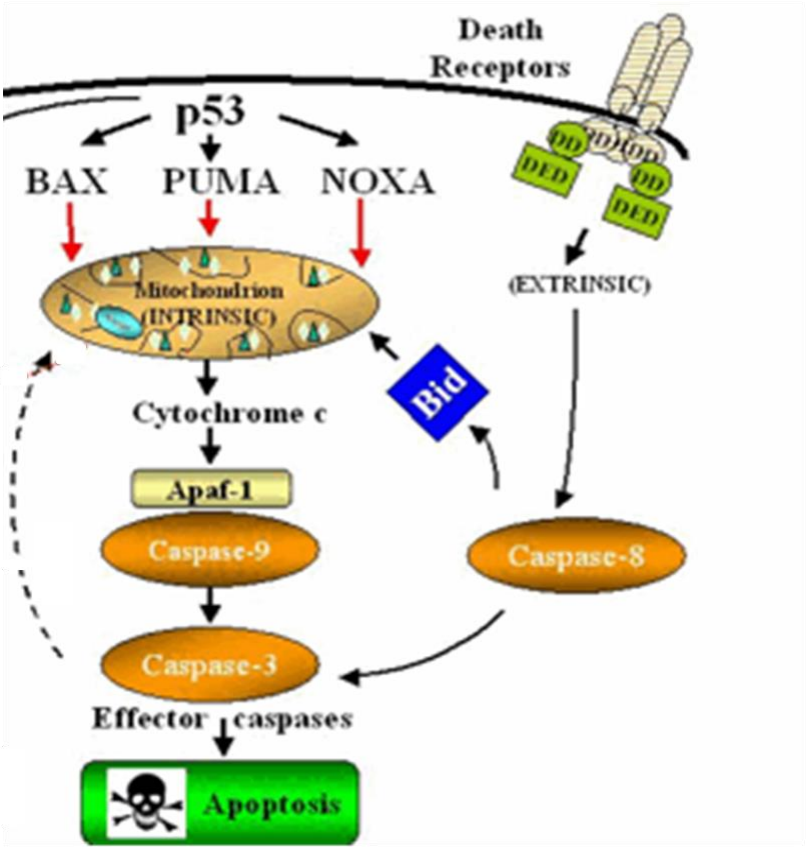

Figure 1.1: p53 mediated apoptosis signaling pathway. DNA damage, aberrant oncogene expression and other stresses signal the activation of kinases (ATM, ATR) which activate p53 through phosphorylation as well as other proteins which inhibit mouse double minute 2 homologue (MDM2) polyubiquitination of p53. The activation and stabilization of p53 leads to transactivation of genes encoding proteins required for apoptosis such as BAX, PUMA and Noxa. P53 is also believed to directly activate BAX. Activation of PUMA, NOXA and BAX lead to the release of cytochrome C from the mitochondria. Cytochrome C then binds to Apaf-1 along with ATP activating Apaf-1 and forming the apoptosome. This complex is then able to cleave pro-caspase9 into its active form Caspase9. This is the initiation step of the Caspase signaling cascade which commits the cell to apoptosis. (Węsierska-Gądek and Schmidt V, 2007; http://www.cancer-therapy.org/CT/v5/B/HTML/25._We%3Fsierska-Ga%3Fdek_and_Schmid,_203-212.html)

1.2.3 Post-translational modification of p53

As previously mentioned p53 is a crucial cell regulatory protein which is constantly being synthesized so that it is ready to respond rapidly to cellular stresses (Kubbutat *et al*., 1997). Therefore, p53 is highly regulated through various combinations of PTMs, with at least 50 different reported modifications including phosphorylation, methylation, acetylation, glycosylation, sumolyation, neddylation and poly-ribosylation (Figure 1.2) (Meek and Anderson, 2009). Many of these modifications have been found to be interdependent (Meek and Anderson, 2009).

When p53 function is not required the E3 ligase mouse double minute 2 homologue (MDM2) polyubiquitinates p53 (Haupt *et al*., 1997). This polyubiquitination targets p53 for proteasomal degradation (Haupt *et al*., 1997). When genotoxic stress is present MDM2 becomes inhibited through a number of mechanisms, including acetylation of p53 (Tang *et al*., 2008). Once MDM2 is inhibited p53 levels rise dramatically (Bates and Vousden, 1996).

The p53 protein is also inhibited by monomethylation on lysine 382 by the lysine methyltransferase Su(var)3-9, Enhancer of Zeste, Trithorax 8 (SET8) (Shi *et al*., 2007) and mono-methylation on lysine 370 by another lysine methyltransferase, lysine methyltransferase 3C (KMT3C) (Huang *et al*., 2006). Methylation at these sites inhibits p53's transactivation activity. As mentioned above, p53 can be activated by phosphorylation of certain residues. The phosphorylation of p53 at Ser15 activates p53 activity and has been found to promote further phosphorylation at other sites enhancing p53 translational activity (Yang *et al*., 2004). Notably, p53 can also be activated by methylation at lysine 372 by Su(var)3-9, Enhancer of Zeste, Trithorax 7/9 (SET7/9) (Chuikov *et al*., 2007).

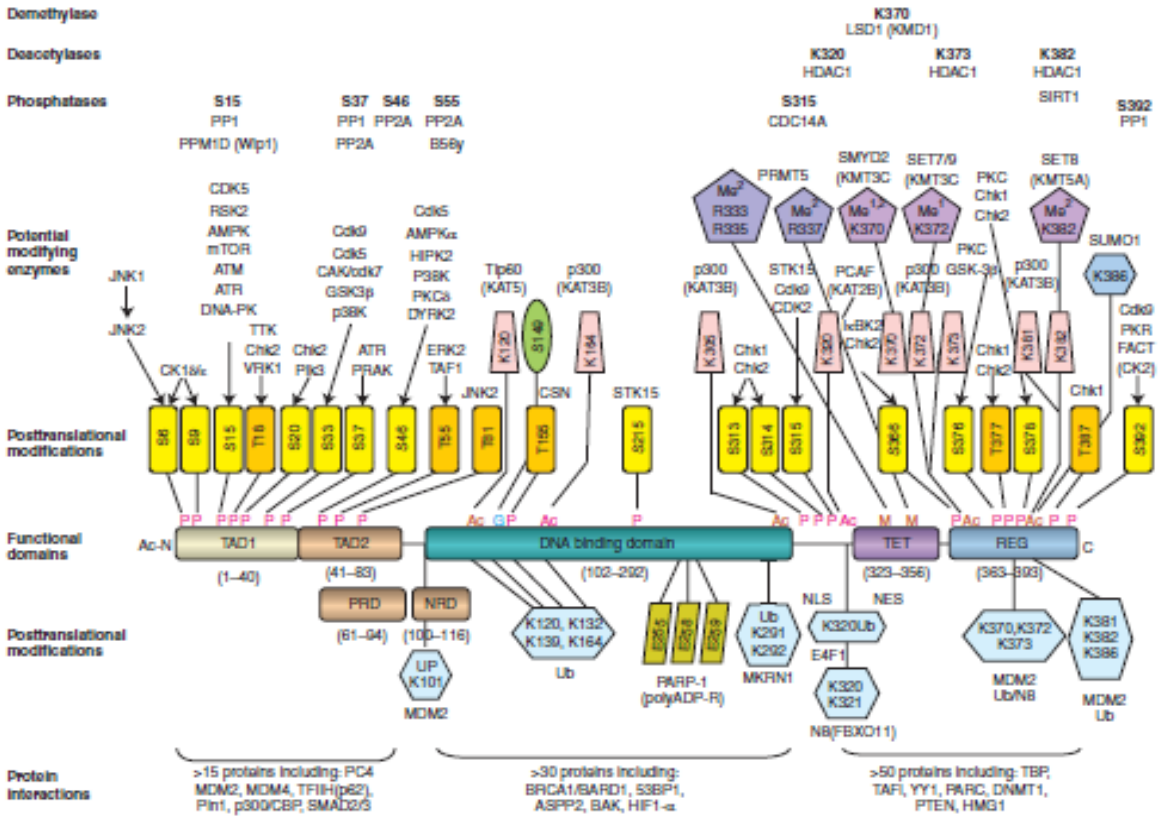

Figure 1.2: Identified post-translational modifications of human p53 and their suspected modifying proteins. The p53 protein undergoes a number of post-translational modifications, including phosphorylation, methylation, acetylation, ubiquitination and glycosylation as shown here. A number of modifying proteins regulate these modifications which lead to p53 activation, inhibition, stabilization or destabilization. (Meek and Anderson, 2009)

1.2.4 Stabilization of p53 by Numb

Numb was originally identified as a cell fate determinant in *Drosophila* embryos during the development of the Drosophila nervous system (Uemura *et al*. 1989). Ten years later, four human Numb isoforms were discovered (Verdi *et al*. 1999). Expression of Numb isoforms has been identified in almost all adult and embryo tissues, suggesting that Numb function is not specific to neuronal development.

Numb has been characterized as an adaptor protein with a wide range of functions including roles in differentiation (Zhong *et al*., 1997), cell polarity and adhesion (Wang *et al*., 2009), cell migration (Nishimura and Kaibuchi, 2007), endocytosis (Santolini *et al*., 2000) and ubiquitination and proteolytic degradation (McGill and McGlade, 2003). Numb interacts with its binding partners via two protein-protein binding domains, an amino terminal phosphotyrosine binding domain (PTB) (Bork and Margolis, 1995; Li et al., 1998; Li *et al*., 1997) and a carboxy-terminal proline rich region (PRR) with Src-homology 3(SH3) binding sites (Yan, 2010). Also at the C-terminus, there are Esp15 homology (EH) regions containing aspartic acid-proline-phenylalanine (DPF) and asparagine-proline-phenylalanine (NPF) motifs (Gulino *et al*., 2010). There have been 9 splice variants identified to date, with isoforms 1-4 the most well-known. Isoform 1 and 3 have predicted molecular weight of 72 and 71 kDa (Numb-PRR_L) respectively and differ from isoform 2 and 4, with a molecular weight of 66 and 65 kDa (Numb-PRR_S) respectively, by an insert of 48 amino acids within Numb's proline rich region (PRR) (Yan, 2010). Isoform 1 and 2 also contain an 11 amino acid insert within the PTB domain which isoform 3 and 4 do not contain (Yan, 2010).

Numb can form binary complexes with MDM2 and p53 (Numb-MDM2 and Numb-p53) (Juven-Gershon *et al*., 1998; Yogosawa, 2008) as well as a tricomplex with both MDM2 and p53 (Numb-MDM2-p53) (Yogosawa, 2008). Numb binding to p53 stabilizes the

protein by inhibiting MDM2 polyubiquitination of p53, so that p53 is no longer targeted for degradation (Yogosawa, 2008). Critically, the Numb-p53 interaction has been shown to be regulated by Numb methylation (Dhami *et al*., 2013). In an unstressed cell, Numb has been shown to be methylated on lysine 158 (K158) and lysine 163 (K163) by the methyltransferase SET8 (Dhami *et al*., 2013). This methylation blocks Numb binding to p53 (Dhami *et al*., 2013). When the cell experiences a stress such as DNA damage, Numb will become demethylated allowing it to bind to and stabilize p53 (Dhami *et al*., 2013). Numb bound p53 is then able to activate target genes required for the induction of apoptosis (Dhami *et al*., 2013) (Figure 1.3).

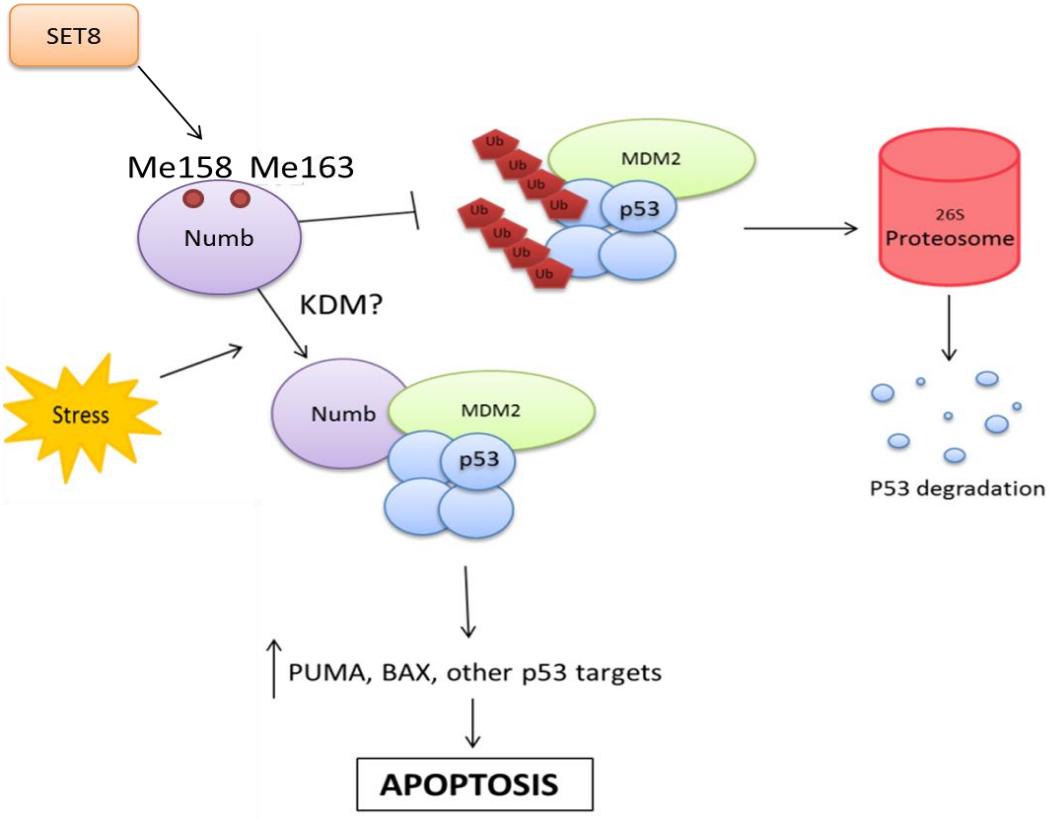

Figure 1.3: The working model of Numb demethylation which leads to stabilization of p53. The lysine demethylase SET8 has been found to methylate Numb. However when the cell experiences a stress signal such as excessive DNA damage or aberrant oncogene expression, an unidentified lysine demethylase (KDM) demethylates Numb. This demethylation allows Numb binding to p53. The binding of Numb to p53 inhibits MDM2 polyubiquitination of p53 which leads to its proteasomal degradation. Stabilization of p53 by Numb binding leads to the up-regulation of pro-apoptotic genes transactivated by p53, which lead to the induction of apoptosis. (Dhami *et al*., 2013)

1.3 The lysine demethylase PHF8

1.3.1 The identification of PHF8

Plant homeodomain finger containing protein 8 (PHF8) is a lysine demethylase (KDM). The *PHF8* gene is located in the Xp11.21 chromosome (Laumonnier *et al*., 2005). It was first identified in 2005 for its association with X linked mental retardation (XLMR) and cleft lip/ cleft lip palate (Laumonnier *et al*., 2005). A mutation in phenylalanine 279 of PHF8 to a serine (F279) is a common mutation seen in patients with XLMR (Koivisto *et al*., 2010). This F279S mutation is located within the catalytic domain of PHF8 and therefore causes the enzyme to have defective demethylase activity. Truncation mutations have also been identified in XLMR patients (Laumonnier *et al*., 2005; Abidi *et al*., 2007). Since PHF8 is largely a nuclear protein, it is thought that these truncating mutations delete putative nuclear localization sequences (NLS) therefore inhibiting PHF8 from entering the nucleus and acting on its target genes (Abidi *et al*., 2007).

Although PHF8 is a ubiquitously expressed protein, murine PHF8 expression levels were found to be high in both the embryonic and adult brain of mice (Laumonnier *et al*., 2005). PHF8 has also been shown to be involved in neuronal differentiation (Qui *et al*., 2010). Exogenous overexpression of PHF8 in the mouse embryonic cell line P19 drove cells towards neuronal differentiation (Qui *et al*., 2010). At least one of the ways PHF8 drives neuronal differentiation is through the retinoic acid receptor alpha (RARα). PHF8 has been found to activate RARα expression as well as act as a co-activator of RARα through direct interaction with the receptor (Qui *et al*., 2010).

1.3.2 Characterization of PHF8

The PHF8 protein is a lysine demethylase that belongs to the largest family of demethylases, the Jumonji C (JmjC) family also known as JmjC histone demethylases (JHDM) (Loenarz *et al*., 2009; Yue *et al*., 2010). Unlike other demethylases, JmjC domain containing proteins are able to remove all three histone methylation states, mono-, di- and tri-methylation (Klose *et al*. 2006). JHDMs catalyze lysine demethylation in an oxidative reaction and they require cofactors α- ketogluterate and

iron [Fe (II)] for the demethylation reaction as demonstrated in Figure 1.4A (Klose *et al*. 2006; Tsukada *et al.*, 2006). Within the JHDM family, PHF8 belongs to the lysine demethylase 7 (KDM7) subfamily containing three members: KDM7A/JHDM1D, KDM7B/PHF8, and KDM7C/PHF2 (Fortschegger and Shiekhattar, 2011). All KDM7 family members seem to target mono- and dimethylated histone H3 lysine 9 (H3K9me1/2), dimethylated histone H3 lysine 27 (H3K27me2) and monomethylated histone H4 lysine 20 (H4K20me1) (Fortschegger and Shiekhattar, 2011).

The PHF8 protein exists in at least 4 different isoforms created by alternate splicing. Isoform 1 is the largest, containing 1060 amino acids and weighing approximately 118kDa (Kikuno *et al*., 1999). Isoform 2 of PHF8 is missing amino acids 1-36 and therefore contains 1024 amino acids (Bechtel *et al*., 2007). Isoform 3 is missing amino acids 478-578 and isoform 4 is missing both amino acids 1-36 and 478-578 but also has an additional 24 amino acids added to the C terminal of the protein (Ota *et al*., 2004). PHF8 contains a PHD zinc finger domain at amino acids 7-53 in isoform 2 (Laumonnier *et al*., 2005) or 43-89 in isoform 1(Kikuno *et al*., 1999). The JmjC domain is located between amino acids 195-294 in isoform 2 (Laumonnier *et al*., 2005) and 231-330 in isoform 1 (Kikuno *et al*., 1999). Both of these domains are highly conserved among PHF8 homologues in other species. PHF8 is a highly conserved protein though evolution with orthologues present in yeast (Laumonnier *et al*., 2005).

The PHD domain of PHF8 is believed to recognize and bind to tri-methylated histone H3 lysine 4 (H3K4me3) (Figure 1.4B)(Feng *et al*., 2010). This binding localizes PHF8 to its target methylated lysines, giving it substrate specificity (Feng *et al*., 2010). The targeting of PHF8 to H3K4me3 suggests that it is involved in promoting transcription as H3K4me3 is a suggested marker for gene activation. Methylated H3K27, H4K20 and H3K9 are all found to repress transcription (Vakoc *et al*., 2006). Since PHF8 removes these methylation marks it can be said that it is involved in transcriptional activation. Previous studies have also showed a direct interaction of PHF8 with the C-terminal domain of RNA polymerase II (PolII) (Fortschegger *et al*., 2010). Both PHF8 and PolII have also been found to bind to Su(var)3-9, Enhancer of

Zeste, Trithorax 1 (SET1) (Liu *et al*., 2010; Ng *et al*., 2003). SET1 methylates H3K4 (Roguev *et al*., 2001), therefore providing PHF8 with its binding site.

Additionally, PHF8 has been found to be a regulator of the cell cycle, specifically in the promotion of the G_2/ M transition (Lim *et al*., 2013). Lim *et al*., (2013) found the levels of PHF8 to be highest at both the G_2 phase and the beginning of M phase. This study found that when PHF8 is knocked down, it results in delayed G_2/ M phase transition and therefore impairs mitosis (Lim *et al*., 2013). Sun *et al*., (2013) discovered that when they knocked down PHF8 there was a decrease in cell proliferation, supporting PHF8's involvement in promoting cell cycle progression. Phosphorylation of PHF8 by cyclin dependent kinase 1(CDK1) has been found to occur on serine 33 and serine 84 causing the dissociation of PHF8 from its bound chromatin (Liu *et al*., 2010). This phosphorylation and subsequent dissociation occurs towards the end of the G_2 phase allowing accumulation of H4K20me1 and progression into mitosis (Liu *et al*., 2010). During interphase PHF8 is recruited to the chromatin again by its interaction with H3K4me3 (Liu *et al*., 2010).

A

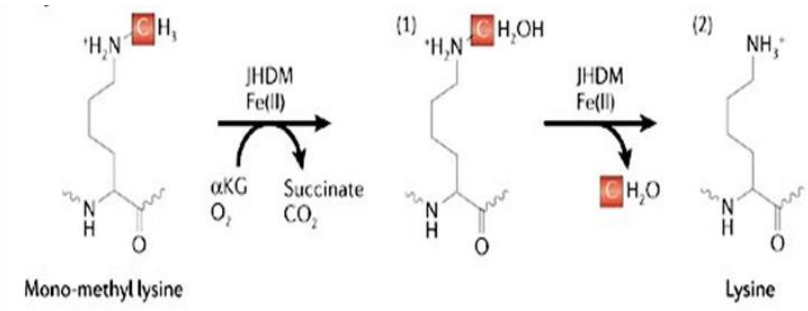

B

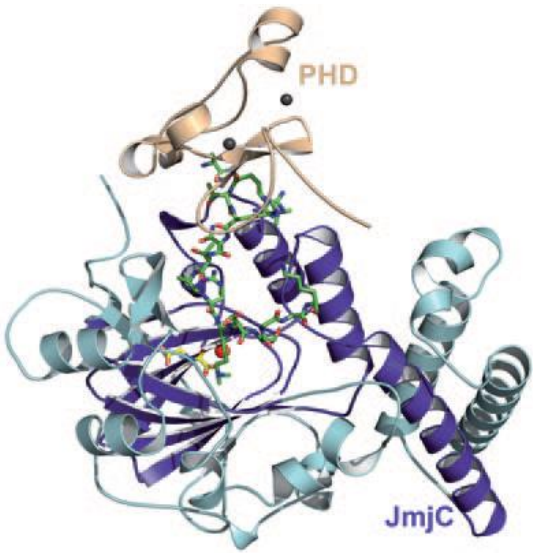

Figure 1.4: The mechanism of PHF8 catalyzed demethylation reaction. A. The lysine demethylase PHF8 requires iron Fe (II) binding and α-ketogluterate as a cofactor for demethylation activity. The methyl group becomes oxidized forming an unstable hydroxymethyl (CH_2OH). This hydroxymethyl group becomes released as formaldehyde (CH_2O), (Klose *et al*., 2006). B. A ribbon model of PHF8 demonstrates binding to a H3K4me3K9me2 peptide (green stick structure). The H3K4me3 is interacting with the PHD domain (cream), while the H3K9me2 is interacting with the JmjC domain (indigo) along with the Fe (II) molecule (red sphere) and α-ketogluterate (yellow stick structure) (Krishnan *et al*., 2011).

1.3.3 Oncogenic properties of PHF8

The PHF8 protein has recently been identified as an oncogenic protein (Bjorkman *et al*., 2012). Elevated PHF8 expression has been reported in many prostate cancer patient samples (Bjorkman *et al*., 2012). PHF8 has also been found to play a role in the pathogenesis of esophageal squamous cell carcinoma (ESCC) (Sun *et al*., 2013). PHF8's oncogenic effects are a result of its ability to promote cell migration, cell cycle progression/cell proliferation and inhibit apoptosis (Bjorkman *et al*., 2012; Sun *et al*., 2013).

PHF8 promotes cell motility by regulating cytoskeletal remodeling as well as up-regulating the expression of genes involved in cell migration such as fibronectin, integrins and proteins involved in the integrin pathway (Bjorkman *et al*., 2012; Asensio-Juan *et al*., 2012). When PHF8 is silenced in prostate cancer cells there is a significant decrease in cell motility (Bjorkman *et al*., 2012). The opposite is seen when PHF8 is overexpressed, cells become more motile (Bjorkman *et al*., 2012). Sun *et al*., (2013) also found that PHF8 knockdown ESCC cells were more motile and invasive then their PHF8 expressing counterparts.

As an example of its oncogenic roles, PHF8 has also been found to promote cancer cell proliferation. Knockdown of PHF8 significantly decreased cell proliferation in prostate cancer cells (Bjorkman *et al*., 2012). One of the ways PHF8 is suggested to affect cell cycle progression is through the demethylation of H4K20 (Liu *et al*., 2010). Methylated H4K20 is a repressive mark found on many of the oncogenic transcription factor E2F, target genes (Abbas *et al*., 2010), and PHF8 binds to E2F1 (Liu *et al*., 2010). PHF8 has also been found to promote cell proliferation in esophageal squamous carcinoma cells (Sun *et al*., 2013). Sun *et al*., (2013) reported that when they knocked down PHF8 they saw significant inhibition of cell proliferation. They also found that both anchorage- dependent and independent growth of ESCC cells were decreased when PHF8 was knocked down (Sun *et al*., 2013). This same study also reported that when prostate cancer cells were injected into nude mice they formed larger tumours than those injected with prostate cancer

cells with PHF8 knocked down by shRNA (Sun *et al*., 2013). This suggests that PHF8 may be a potential target for cancer therapeutics.

Finally, an effect of PHF8 on apoptosis has also been identified. Bjorkman *et al*., 2012 report a weak yet significant effect on apoptosis in cells with PHF8 knocked down. Knockdown of PHF8 in ESCC cells was also found to significantly increase apoptosis (Sun *et al*., 2013). Although PHF8 has been found to negatively affect apoptosis, there has been no research done to investigate the mechanism behind its anti-apoptotic effect.

1.4 The purpose of this thesis

It is known that Numb is methylated by SET8 at sites K158 and K163; however the protein responsible for demethylating Numb remains unknown. The purpose of this thesis was to determine which lysine demethylase is demethylating Numb. We identified PHF8 as a possible candidate for the Numb demethylase since it targets methylated H3K27 and H4K20 which share sequence similarities to Numb K159 and K163 (Dhami *et al*., 2013). Previous research has indicated PHF8 as an oncogene; therefore it would be of interest to further investigate any possible roles for the lysine demethylase in regulating p53 mediated apoptosis.

We hypothesize that PHF8 demethylation activity plays a regulatory role in the intrinsic p53-mediated apoptosis pathway.

Aim 1: Identify and characterize candidate Numb demethylases

To address this aim we selected possible demethylases by identifying demethylases known to target lysines on histone tails with similar surrounding sequences to Numb K158 and K163. The chemotherapeutic drug, doxorubicin, was used to induce apoptosis and the levels of mRNA of these demethylases were observed during apoptosis to see if there were any changes compared to non-apoptotic/ untreated cells. SET8 levels have been found to decrease when cells undergo apoptosis, so we

suspected that the potential Numb demethylase levels would increase when apoptosis is induced.

Aim 2: Observe the effect of PHF8 on apoptosis

To address this second aim, flow cytometry analysis was done to observe the effect of PHF8 on apoptosis. PHF8 was either overexpressed or knocked down and the levels of apoptosis were observed. Quantitative real time-PCR (qRT-PCR) was used to observe any effect PHF8 has on genes involved in apoptosis. The mRNA levels of the apoptotic proteins were observed in cells with PHF8 overexpressed and in cells with PHF8 knocked down. Chromatin immunoprecipitation (ChIP) was also done to determine if PHF8 is directly regulating the promoters of the observed apoptotic genes it seemed to have an effect on. ChIP analysis was also done with H3K27me3 immunoprecipitated from cells overexpressing PHF8 and cells with PHF8 knocked down, to determine if PHF8 was regulating the genes through the methylation status of H3K27.

Chapter 2

2 Materials and Methods

2.1 Solutions and buffers

All solutions and buffers used are listed here in table 2.1.

Table 2.1: Solutions and buffers

Solution	Components
1×TAE buffer (pH8.5)	Tris base 40 mM, EDTA 1 mM, Glacial acetic acid adjusting pH to 8.5
1× TBST	Tris base 20 mM, NaCl 137 mM, Tween20 0.05% (v/v)
1× PBS buffer	KH_2PO_4 1 mM, Na_2HPO_4 10 mM, KCl 2.7 mM, NaCl 137 mM
5× SDS-PAGE (Laemmli) Sample buffer	Tris base (pH 6.8) 312 mM, SDS 10%, α-mercaptoethanol 25%, Bromophenol Blue 0.05%, Glycerol 50%
Western blot transfer buffer	Methanol 20%, 24 mM Tris base, 194 mM Glycine
1x MOPS buffer	50 mM MOPS, 50 mM Tris base, 0.1% SDS, 1 mM EDTA
ChIP SDS lysis buffer	1% SDS, 10 mM EDTA, 50 mM Tris (pH 8.1)
ChIP dilution buffer	0.01% SDS, 1% Triton X-100, 1.2 mM EDTA, 16.7 mM Tris-HCL (pH 8.1), 167 mM NaCl
LiCl wash	0.25 M LiCl, 1% IGEPL-CA630, 1% deoxycholic acid (sodium salt), 1mM EDTA, 1 mM Tris (pH8.1)
High salt wash	0.1% SDS, 1% Triton X-100, 2 mM EDTA, 20 mM Tris-HCL (pH8.1), 500 mM NaCl
Low salt wash	0.1% SDS, 1% Triton X-100, 2 mM EDTA, 20 mM Tris-HCL (pH8.1)
TE pH 8.0	10 mM Tris-HCl, 1 mM EDTA (pH adjusted with HCl)

2.2 Cell culture, transfection and siRNA knock down

2.2.1 Cell culture

HeLa cells a cervical cancer cell line and U2OS cells, an osteosarcoma cell line, were grown in Dulbecco's modified Eagle's medium with 10% fetal bovine serum (FBS) and 2 mg/ml glutamine at 37 ℃ with 5% CO_2.

2.2.2 Cell transfection

Cells were subcultured the day prior to the transfection to be 50-80% confluent in a 100 mm tissue culture dish. 8 µg of DNA was mixed with 440 µl warm Opti-MEM (Life Technologies) and incubated at room temperature for 5 minutes. 60 µl (1 mg/ml) warm Polyethylenimine (PEI) was then added to the diluted DNA and mixed immediately for 15 seconds. The solution was left for 20 minutes at room temperature prior to adding it to the cells. Before the addition of DNA to the cells, cells were washed three times with warm 1 x phosphate buffered saline (PBS) and cells were left in 4.5 mL antibiotic free media. 24 hours after the addition of the DNA solution to the cells, cells were washed three times with warm 1 x PBS and 10 mL of fresh media was added to the plate. Cells were then grown for another 18-24 hours prior to use.

2.2.3 SiRNA transfection

Cells were subcultured the day prior to the transfection to be 40-70% confluent. 10 µl of 100 µM siRNA (Sigma-Aldrich) was diluted in 990µl serum free media and incubated at room temperature for 5 minutes. 20 µl DharmaFECT (ThermoFisher Scientific, Catalogue #T-2001-01) was diluted in 980 µl serum free media and also incubated at room temperature for 5 minutes. The two were then mixed together and incubated at room temperature for 20 minutes. Cells were washed three times with 1 x PBS then replenished with 8 ml of antibiotic free media. The siRNA mixture was then added to the cells and incubated at standard conditions for 48 hours.

2.2.4 Doxorubicin treatment

Cells were treated with 1 µM doxorubicin hydrochloride (Sigma-Aldrich, Catalogue # D1515-10MG) dissolved in ddH_2O for 18 hours at 37°C. Doxorubicin was added directly to cell culture media. For a 100 mm dish with 10 ml of media, 2 µl of 5 mM doxorubicin stock was used.

2.3 Quantitative real-time polymerase chain reaction (qRT-PCR)

2.3.1 TRIzol RNA isolation

Cells were grown in 6-well dishes, 2 wells per condition. Cells were transfected on day one, media changed and doxorubicin was added on day 2 for an 18 hour treatment. Media was aspirated and 600 µl of TRIzol (Life Technologies, Catalogue#15596-026) was added per well. Cells were scraped off the dish in TRIzol and collected in micro-centrifuge tubes and the mixture was pipetted up and down a few times. Cells were left at room temperature for 5 minutes prior to the addition of 120 µl chloroform. Tubes were shaken vigorously for 15 seconds and left at room temperature for 3 minutes. Samples were then centrifuged for 15 minutes at 4°C at 12 000 x g. The upper aqueous phase was transferred to a new centrifuge tube and 300 µl isopropanol was added and left at room temperature for 10 minutes to precipitate the RNA. The precipitated RNA was the pelleted by centrifugation 12 000 x g for 10 minutes at 4°C. The RNA pellet was then washed with 1 mL 75% ethanol and centrifuged again for 5 minutes 12 000 x g at 4°C. The ethanol was aspirated away and the pellet was left to air dry for 5 to 10 minutes. The RNA was re-suspended in DEPC treated water (RNase-free) by pipetting up and down several times and incubating 15 minutes in a 55°C water bath. RNA concentration was calculated by measuring absorbance A_{260} and using the following formula $A260x\ dilutionx40 = \frac{\mu gRNA}{mL}$. Absorbance at A_{280} was also measured and the ratio A_{260}/A_{280} was calculated to ensure a ratio >1.8. Samples were either stored at -80°C or used for cDNA synthesis for qPCR.

2.3.2 cDNA synthesis

Isolated RNA was reverse transcribed since cDNA is more stable than RNA. BioRad's iScript™ Reverse Transcription Supermix for RT-qPCR was used (Bio-Rad, Hercules, CA, Catalogue # 170-8840). 500 ng-1 µg of RNA was used depending on the concentration of each sample. For each set of experiments the RNA concentration was adjusted so all samples were at the same concentration. 2 µl of RNA solution was added to 4 µl 5x iScript reverse transcription supermix (Bio-Rad, Hercules, CA, Catalogue # 170-8840) and14 µl of water for a final volume of 20 µl for each sample. The reaction mixtures were prepared in PCR tubes. In a PCR thermocycler (iCycler- Biorad, Hercules, CA) the following protocol was used for cDNA synthesis: 5 minutes at 25°C, 30 minutes at 42°C, 5 minutes at 85°C and a final hold at 4°C. A no-RT control was also done to exclude genomic DNA contamination.

2.3.3 qRT-PCR procedure

iQ™ SYBR® Green Supermix (Bio-Rad, Hercules, CA, Catalogue # 170-8884) was used for RT-qPCR reactions performed in the Bio-Rad CFX connect Real-Time system (Bio-Rad, Hercules, CA). iQ™ SYBR® Green Supermix contains iTaq DNA polymerase, dNTPs, $MgCl_2$, SYBR® Green I dye, fluorescein as well as enhancers and stabilizers. Each reaction was a final volume of 10 µl consisting of 4 µl cDNA and 0.2 µl forward primer, 0.2 µl reverse primer, 0.6 µl nuclease free H20, 5 µl SYBR Green supermix. The forward and reverse primers, nuclease-free H_2O and SYBR Green were combined into a master mix and 6 µl of mater mix was added to the cDNA. The reactions were carried out with the following parameters:

Cycle 1: Denaturation: 95°C 3 minutes

Cycle 2 (40-50 x): Denaturation: 95°C 10 seconds

Annealing/extension: 60°C 30 seconds

Finally samples were heated from 65°C to 95°C in 0.5°C increments every 5 seconds to create a melt curve. Further analysis such as normalization, graphs and statistics were done using Microsoft Excel.

2.3.4 qRT-PCR primers

Primers used in this study for qPCR analysis were designed using the National Center for Biotechnology Information's (NCBI) Primer-BLAST search and ordered from Sigma Aldrich. The sequences for the primers used can be found in Table 2.2.

Table 2.2: List of qRT-PCR primers

Gene	Forward primer	Reverse primer
SETD8	GGGGAAACCATTAGCCGGAA	TGTTCCTCGGACTTCATGGC
KDM6B	TGAAGAACGTCAAGTCCATTG	TCCCGCTGTACCTGACAGT
KDM6A	ATGGAAACGTGCCTTACCTG	ATTAGGACCTGCCGAATGTG
PHF8	TAGCACAGGGCACAAGGTTC	CGATAGGCTGGGCTCTTTCC
TP53	GAGGTTGGCTCTGACTGTACC	TCCGTCCCAGTAGATTACCAC
BAX	TTTGCTTCAGGGTTTCATCC	CAGTTGAAGTTGCCGTCAGA
CASP3	TGAGGCGGTTGTAGAAGAGTT	TGAACCAGGAGCCATCCTTT
PUMA	GCCAGATTTGTGAGACAAGAG G	CAGGCACCTAATTGGGCTC
Rpl13	GCCCTACGACAAGAAAAAGCG	TACTTCCAGCCAACCTCGTGA
GAPDH (ChIP)	CAATTCCCCATCTCAGTCGT Nucleotides region 467-482	TAGTAGCCGGGCCCTACTTT Nucleotides region 654-673
BAX (ChIP)	TTTGCTTCAGGGTTTCATCC Nucleotides region 144-163	CAGTTGAAGTTGCCGTCAGA Nucleotides region 370-389
TP53 (ChIP)	CAGCACATGACGGAGGTTGT Nucleotides region 562-581	TCATCCAAATACTCCACACGC Nucleotides region 666-686

CASP3 (ChIP)	TGAGGCGGTTGTAGAAGAGTT Nucleotides region 65-85	TGAACCAGGAGCCATCCTTT Nucleotides region 890-909

2.4 Transformation of *Escherichia coli* (*E. coli*) and DNA plasmid amplification

500 ng – 1 µg of plasmid DNA (Table 2.3) was added to a microcentrifuge tube on ice. *E. coli* DH5α cells were thawed on ice. 30 µl of the competent cells were added to the DNA and mixed by gently pipetting up and down several times. The cells and DNA were incubated on ice for 15 minutes. The bacteria/plasmid mixture was then heat shocked at 42°C for 60 seconds, followed by incubation for 2 minutes on ice. 70 µl of antibiotic free LB media was added to the bacteria and plasmid mixture and was incubated at 37°C on a shaker for one hour.

DH5α cells were then plated on agar plates with the appropriate antibiotic resistance. pFLAG-CMV constructs confer ampicillin resistance, therefore 50 µg/ml ampicillin agar plates were used. Plates of bacteria were left to grow overnight at 37°C. The next day colonies were picked and grown in 3 ml LB media with the appropriate antibiotic. Cell cultures were left to grow overnight at 37°C on a shaker.

Plasmid DNA was purified using a miniprep DNA plasmid purification kit (Sigma-Aldrich, St. Louis, MO, USA).

Table 2.3: List of plasmids

Plasmid	**Protein**	**Host**	**Source**
pFLAG-CMV2	Empty vector with FLAG tag	*E.coli* DH5α	Li lab
pFLAG-hPHF8-CMV2	Human PHF8 isoform 2	*E.coli* DH5α	Li lab (Courtney Voss); The ORFeome Collaboration (hPHF8 insert)

2.5 Cell extract preparation, immunoprecipitation and western blot

2.5.1 Cell lysis

Cells were placed on ice and washed three times with ice cold 1 x PBS. 500 µl-1 mL lysis buffer (Table 2.1) supplemented with 1 mM sodium orthovanadate, 2 µg/ml aprotinin, 10 µM leupeptin, 1 µM E64, 1 µM bestatin, 1 µM pepstatin A and 1 mM phenylmethanesulfonyl fluoride (PMSF) was added to the 100 mm dish of cells and left on ice for 5 minutes. Cells were then scraped into a 1.5 ml Eppendorf tube using a rubber policeman on ice. The cell lysates were rotated for 15 minutes at 4°C prior to centrifugation at max speed (16000 x g) for 20 minutes at 4°C. The supernatant was removed and used for subsequent experiments.

2.5.2 Measurement of protein concentration

Protein concentration was measured using Bradford dye assay (Bio-Rad protein assay). The dye was diluted in a 1 part dye to 4 parts ddH_20 ratio. 1-2 µl of sample was added to 800µl of diluted dye in a plastic cuvette. The absorbance was measured in a GENESYSTM spectrophotometer (Spectronic Unicam, Rochester, NY, USA) at a wavelength of 595 nm. Protein concentration of the sample was determined using a bovine serum albumin (BSA) standard curve.

2.5.3 Measurement of DNA and RNA concentration

5 µl of DNA or RNA sample was added to 495 µl ddH_20 in a glass cuvette. 500 µl ddH_20 was used as a blank. Both DNA and RNA samples were measure at 260 nm absorbance. DNA concentration was calculated using the formula: $A260\ x\ dilution x\ 50 = \frac{\mu gDNA}{mL}$. RNA concentration was calculated using the formula: $A260 x\ dilution x 40 = \frac{\mu gRNA}{mL}$. Absorbance was also read at 280 nm to get the 260 nm/280 nm ratio.

2.5.4 Immunoprecipitation (IP)

To pre-clear the cell lysate 3 µg of anti-rabbit IgG was added to 1 mg total protein cell lysate. 40 µl of a 1:1 ratio mixture of protein A agarose beads (made in lab) to lysis buffer was added to the cell lysate with anti-IgG and incubated for one hour at 4°C on a shaker. Samples were centrifuged at 4°C 3000 x g for 5 minutes and the supernatant was transferred to a new 1.5 ml Eppendorf tube.

3 µg of antibody for IP per 1 mg of total protein was then added to the pre-cleared lysate and incubated at 4°C on a shaker for 4 hours or overnight. 40 µl of protein A bead slurry in lysis buffer was added to each sample and incubated another hour at 4°C on a shaker. Samples were then centrifuged for 5 minutes 3000 x g at 4°C. Supernatant was removed and beads with the antigen and protein attached were washed three to five times with cell lysis buffer. After the last wash, supernatant was removed and 2 x SDS Laemmli sample buffer was added to the beads to elute the protein.

2.5.5 Western blot (WB)

20-40 µg of protein sample was loaded onto a 8-12 % Bis-Tris gel. Gels were run in 1 x 3-(N-morpholino) propanesulfonic acid (MOPS) buffer (Table 2.1) at 110 V for approximately one to two hours. The separated proteins were then transferred onto a polyvinylidene fluoride (PVDF) membrane solubilized in methanol. A semi-dry blot transferring system (BioRad, Hercules, CA) was used to transfer the gel at 21 V for 30 minutes. The gel and PVDF membrane were placed between two filter papers soaked in 1 x transfer buffer (Table 2.1).

Following the transfer, PVDF membranes were blocked in either 5 % skim milk in 1 x Tris-buffered saline with Tween (TBST) or 3% bovine serum albumin (BSA) in 1 x TBST for one hour at room temperature on a shaker. The blocking buffer was removed and the membrane was incubated with primary antibody diluted in blocking buffer for one hour on a shaker at room temperature or overnight at 4°C on a shaker. The dilution of primary antibody used was in accordance to the recommended dilution given by the manufacturer (Table 2.3).

After the primary antibody was removed, the membrane was rinsed three times with 1 x TBST then washed 3 x 5 minutes with 1 x TBST. Next the membrane was incubated in secondary antibody conjugated with horseradish peroxidase (HRP) diluted in a ratio of 1:5000 in 5% skim milk in 1 x TBST for one hour. The membrane was then rinsed three times and washed 3x 15 minutes with 1 x TBST. An enhanced chemiluminescence (ECL) detection solution (GE Healthcare Life Sciences) was added to the membrane and incubated for 5 minutes. Excess ECL solution was removed and signals were exposed onto X-ray film over a range of 15 seconds to 15 minutes. Film was then developed using a Kodak M35A X-OMAT processor.

Table 2.4: List of antibodies

Antibody	**Species**	**Source**	**Conditions**
Numb (H-70)	rabbit	Santa Cruz Biotech (Catalogue number: sc-25668)	1:1000 dilution in 5% milk in 1xTBST
PHF8 (ab36068)	rabbit	Abcam (Catalogue number:ab36068)	1:1000 dilution in 5% milk in 1xTBST
p53(DO-1)	mouse	Santa Cruz Biotech (Catalogue number: sc-126)	1:1000 dilution in 5% milk in 1xTBST
β-tubulin (H-235)	rabbit	Santa Cruz Biotech (Catalogue number: sc-9104)	1:1000 dilution in 5% milk in 1xTBST
FLAG (M2)	mouse	Sigma Aldrich (Catalogue number: F3165)	1:1000 dilution in 5% milk in 1xTBST
Pan-lysine mono- and di- methylation	rabbit	Abcam (Catalogue number: ab23366)	1:1000 dilution in 3% BSA in 1xTBST

H3K27me3	mouse	Abcam (Catalogue number: ab6002)	N/A

2.6 Flow cytometry analysis

Cells were plated on day 0, transfected with pFLAG-PHF8-CMV or pFLAG-CMV empty vector on day 1, media changed and treated with doxorubicin or not on day 2. On day 3 cells were rinsed with 1 x PBS and trypsinized to remove the cells from the dish. The cells were collected and centrifuged at 1000 x g for 5 minutes and the supernatant removed. An Annexin V-FITC apoptosis detection kit (BioVision incorporated, Cat. # K101-100) was used to detect apoptotic cells according to the manufacturer's protocol. Cells were re-suspended in binding buffer at a concentration of approximately $5x10^5$ cells/ 500 µl. Cells were then passed through a cell strainer to prevent large clumps of cells from clogging the machine. 5 µl of each Annexin V-FITC and propidium iodide (PI) were added to each experimental sample and incubated at room temperature for 10 minutes before being placed on ice. Control tubes were also set up containing no dye, PI alone Annexin V-FITC alone, and both PI and Annexin V-FITC. An unstained non-doxorubicin treated sample was also used to observe the effect of doxorubicin on the emission spectra.

Cells were analyzed on the LSRII flow cytometer (BD Bioscience) using FACS Diva software (BD Bioscience) in Robarts Research Facility. AnnexinV FITC samples were excited by the 488 nm blue laser and detected by the 530/30 detector. For PI stained cells the yellow-green 561 nm laser was used to excite samples and the 610/20 detector was used to detect the fluorochromes. Data analysis was done using FlowJo software (FlowJo Enterprise) and Microsoft Excel.

2.7 Chromatin immunoprecipitation (ChIP) assay

Cells were plated on day 0, transfected with pFLAG-PHF8-CMV or pFLAG-CMV empty vector on day 1, media changed and treated with doxorubicin or vehicle ddH_2O on day 2. On day 3, 270 µl of 37% formaldehyde was added to each 100 mm dish of cells containing 10 ml of media. Cells were incubated with the formaldehyde on a shaker at room temperature for 10 minutes to allow cross-linking of chromatin bound proteins to the nucleotides. 687.5 µl of 2 M glycine was added to the media to quench the cross-linking. The medium mixture was them removed and cells were washed with cold 1 x PBS containing protease inhibitors. 1 ml of cold 1 x PBS plus protease inhibitors was added to the cells and scraped into microcentrifuge tubes. Cells were centrifuged at 3000 x g at 4°C for 5 minutes. Supernatant was removed and the cell pellet was re-suspended in 200 µl ChIP lysis buffer (Table 2.1). Cells were incubated at room temperature for 5 minutes prior to being put on ice. 1.2 ml ChIP dilution buffer (Table 2.1) was added to each sample. Next the lysed cells were sonicated (60 Sonic Dismembrator, Fisher Scientific) for 5 x 15 second on 45 seconds off pulses on number 5. 40 µl of a mixture of 0.2 mg/ml sheared salmon sperm DNA (ssDNA) in ChIP dilution buffer and protein G sepharose beads at a 1:1 ratio was added to the lysate and incubated at 4°C on a nutator to pre-clear the sample. Samples were centrifuged for 2 minutes at 3000 x g 4°C and supernatant transferred to new tubes. 100 µl of supernatant was saved from each sample for ChIP input DNA for normalization. 3 µg of antibody was added to the samples and incubated overnight on a nutator at 4°C. 40 µl of Protein G sepharose/ ssDNA bead slurry was added to each sample and incubated at 4°C for 1 hour on a nutator. Samples were centrifuged 4 minutes at 3000 x g at 4°C. Supernatant was removed and beads were washed with 1 ml low salt buffer (Table 2.1) for 30 minutes, then high salt buffer (Table 2.1) for 15 minutes, then LiCl buffer (Table 2.1) for 10 minutes. Each of these washes was at 4°C on a nutator with centrifugation at 3000 x g at 4°C between to remove each wash. The final two washes were in TE buffer (pH 8.0) (Table 2.1) at room temperature for 5 minutes each. The sample was eluted off the beads using 100 µl 1% SDS and 0.1 M $NaHCO_3$ in ddH_2O. Samples were incubated on a shaker at room temperature for 4 hours then centrifuged for 1 minute at 3000 x g and supernatant kept. Elutant was incubated at 65°C overnight to de-crosslink DNA along with the ChIP input samples.

DNA was purified from the sample using QIAEX II Gel Extraction kit (Qiagen, Venlo, Limburg, Netherlands, Catalogue #20021) following the manufacturer's protocol to extract DNA from solutions. DNA fragments were analyzed using qRT-PCR.

Chapter 3

3 Results

3.1 Prediction of possible Numb demethylases

The original goal of this study was to identify the lysine demethylases responsible for demethylating Numb. Numb has been shown to be methylated by the lysine methyltransferase SET8 on lysine residues K158 and K163 (Dhami *et al*., 2013). The first step in identifying SET8 as the possible lysine methyltransferase targeting Numb was to look at the peptide sequence surrounding the two methylation sites (Dhami *et al*., 2013). Dhami *et al*., 2013 preformed a sequence alignment and found that the sequence was closely related to histone H3 lysine 27 (H3K27) and histone H4 lysine 20 (H4K20), as well as the p53 lysine 382 (p53K382) methylation site (Dhami *et al*., 2013). The latter two are known targets of SET8 (Nishioka *et al*., 2002; Shi *et al*., 2007). Table 3.1 shows the protein sequences surrounding the lysines of interest targeted for methylation.

Since H3K27 and H4K20 were found to have similar surrounding sequences to those of the Numb K158 and K163 residues (Dhami *et al*., 2013), we narrowed down the possible lysine demethylase by identifying demethylases known to target H3K27 and H4K20. We decided to investigate lysine demethylase 6B (KDM6B) and lysine demethylase 6A (KDM6A) which both demethylate H3K27 (Lan *et al*., 2007; Hong *et al*., 2007). In addition to the KDM6 demethylases, plant homeodomain (PHD) finger containing protein 8 (PHF8) which is known to demethylate monomethylated H4K20 (Lui *et al*., 2010) and dimethylated H3K27 (Loenarz *et al*., 2010) was also investigated.

3.2 PHF8 expression increases during doxorubicin induced apoptosis

In order to test which of the suspected lysine demethylases may be demethylating Numb we first looked at which of those demethylases are elevated during apoptosis. The Numb methyltransferase, SET8, has previously been found to be down regulated in cells undergoing apoptosis (Dhami *et al*., 2013), therefore we suspected that the possible Numb demethylase would be up-regulated when apoptosis is induced. Quantitative real

Table 3.1: Sequence comparison of Numb lysine methylation sites to histones and p53 methylation sites. H3K27 and H4K20 were previously identified by sequence alignment to have similar sequence similarity of residues surrounding the methylated lysine as Numb K158 and K163. The methylated lysine K382 of p53 was also identified to have a similar sequence to both Numb methylation sites, H3K27 and H4K20. The alignment gave a score to each of the lysine residues based on sequence similarity of the surrounding amino acids compared to those of Numb (K158). (Dhami *et al*., 2013)

Protein	**Sequence containing lysine methylation site**	**Alignment Score**
hNumb	143-HAVGCAFAACLERKQKREKECGVTATFDAS-174	N/A
H4K20	1-GRGKGGKGLGKGGAKRHRKVLRDNIQGITKPA-34	2.5
p53K382	363-HSSHLKSKKGQSTSRHKKLMFKTEGPDSD-393	1.5
H3K27	10-TGGKAPRKQLATKAARKSAPATGGVKKPH-40	1.5

time polymerase chain reaction (qRT-PCR) was used to identify elevated lysine demethylases. U2OS cells were either untreated or treated with 1.0μM doxorubicin for 18 hours to induce apoptosis. Cells were lysed and the total mRNA was extracted. PUMA, a protein involved in p53 mediated apoptosis was also selected as a positive control since its expression is known to increase when treated with doxorubicin (Dhami *et al*., 2013). SET8 was observed as a negative control since it has been found to decrease with doxorubicin treatment (Dhami *et al*., 2013).

As shown in Figure 3.1, the levels of KDM6A remained relatively constant with the 18 hour doxorubicin treatment compared to the untreated cells. The level of KDM6B mRNA however, decreased significantly with doxorubicin treatment. The only lysine demethylase tested whose levels increased significantly was PHF8. As expected, PUMA levels increased with doxorubicin treatment, well SET8 levels of mRNA decreased.

To further confirm the observed increase in PHF8 expression during apoptosis, we repeated the experiment in HeLa cells (Figure 3.2). Once again the levels of PHF8 were significantly elevated with 18 hours of doxorubicin treatment compared to untreated cells. SET8 was used again as a negative control, which was significantly decreased in both cell lines.

Although the mRNA levels of a gene may be elevated, it does not always result in elevated protein levels. Therefore our next step was to observe the protein expression level of PHF8 with doxorubicin treatment. To test this, cells lysates of both HeLa and U2OS cells treated with doxorubicin for 6 hours, 18 hours or left untreated, were analyzed by western blot (Figure 3.3). Both cell lines showed an increase in PHF8 expression level at 18 hours compared to untreated cells (Figure 3.3, top panels). Numb and p53 expression levels were also observed. Both Numb and p53 expression levels also increased in both cell lines with doxorubicin treatment (Figure 3.3, middle panels).

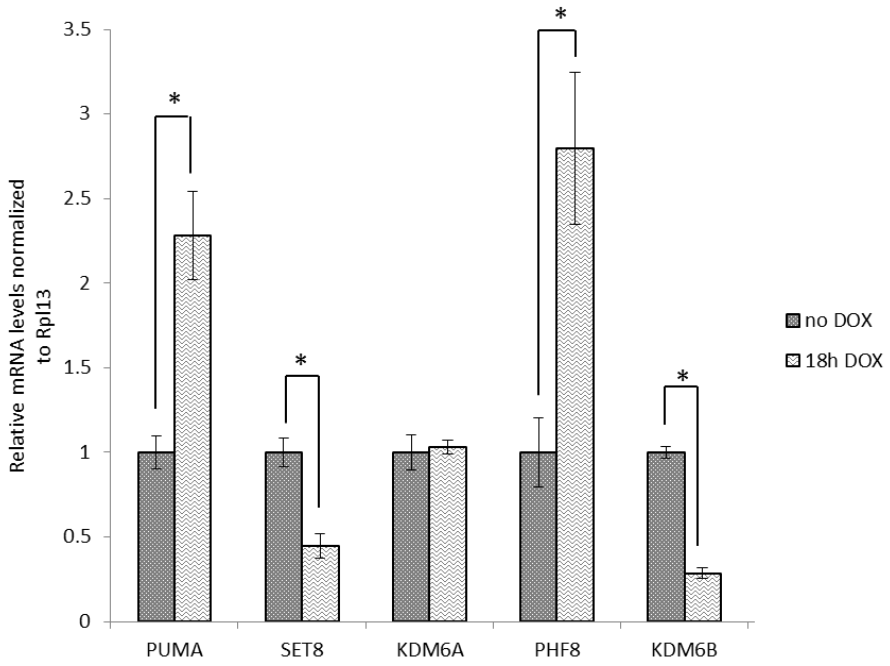

Figure 3.1: Transcript expression levels of lysine demethylases with doxorubicin treatment. Total mRNA was extracted using TRIzol, from U2OS cells treated with 1.0μM doxorubicin for 18 hours. The mRNA was reverse transcribed into cDNA. Primers targeting lysine demethylases were used to analyze levels of demethylase mRNA. SET8 was used as a negative control and PUMA was used as a positive control. Data presented is the mean ± SEM of three biological repeats. *- indicates significant difference from the corresponding control ($p<0.05$).

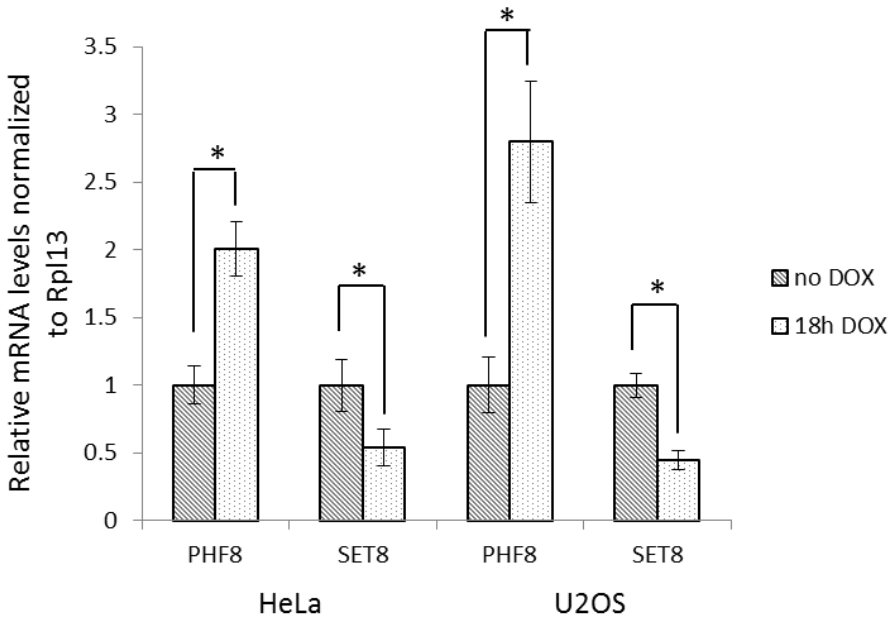

Figure 3.2: Transcript expression of PHF8 increased with doxorubicin treatment in both HeLa cells and U2OS cells. Total mRNA was extracted using TRIzol, from U2OS cells treated with 1.0 μM doxorubicin for 18 hours or from untreated cells. The mRNA was reverse transcribed into cDNA. Primers targeting PHF8 and SET8 were used to analyze levels of mRNA using qPCR. Values were normalized to Rpl13. Data presented is the mean ± SEM of three biological repeats. *- indicates significant difference from the corresponding control ($p<0.05$).

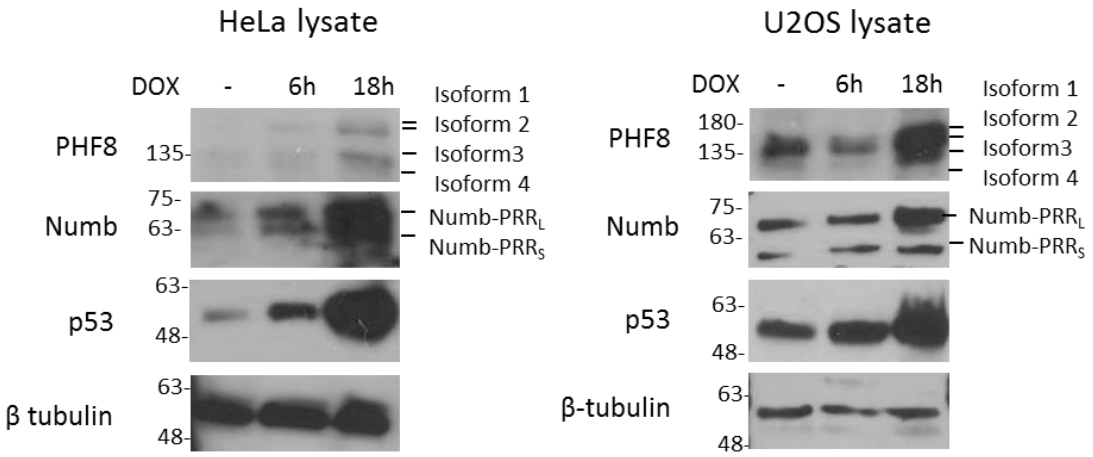

Figure 3.3: PHF8 protein expression level was up-regulated with doxorubicin treatment for 18h. Both HeLa cells and U2OS cells were either left untreated or treated with 1.0μM doxorubicin for 6 hours or 18 hours. Cells were lysed and samples were separated using an 8% Bis-Tris gel. Western blot analysis was done using anti-PHF8 (upper panel), anti-Numb (second panel), anti-p53 (third panel) and anti-β-tubulin (bottom panel). β-tubulin was observed as a loading control to ensure equal levels of protein were added.

3.3 PHF8 does not demethylate Numb

The significant increase in PHF8 mRNA (Figure 3.1 and Figure 3.2) and protein levels during apoptosis (Figure 3.3) led us to believe it could be the demethylase responsible for demethylating Numb. To further test this prediction we set out to observe whether or not PHF8 has an effect on Numb methylation. To do this we overexpressed pFLAG-PHF8-CMV or pFLAG-CMV empty vector in HeLa cells and immunoprecipitated endogenous Numb. Cells were either treated with 1.0μM doxorubicin or left untreated. Numb immunoprecipitated samples along with cell lysates were observed using SDS-PAGE and western blot analysis. As seen in Figure 3.4 A, PHF8 appears to have no effect on Numb methylation status.

3.4 PHF8 has an anti-apoptotic function

Since PHF8 expression increases with doxorubicin induced apoptosis, we predicted that PHF8 would promote apoptosis. To test this hypothesis we used flow cytometry analysis. We first observed cells with PHF8 knocked down using siRNA specific to PHF8. As a control we also observed cells transfected with a scrambled control siRNA. Cells were treated with 1.0 μM doxorubicin for 18 hours or left untreated. Cells were analyzed using Annexin V FITC to observe cells in early apoptosis and propidium iodide (PI) was used to analyze cells in late apoptosis. A significantly higher percentage of cells with PHF8 knocked down were undergoing apoptosis when treated with doxorubicin compared to cells containing the scrambled control siRNA (Figure 3.5). Even untreated PHF8 knockdown cells showed slightly more apoptosis than control cells, however this was not significant.

To further confirm that PHF8 promotes cell survival, HeLa cells were transfected with FLAG tagged PHF8 to observe how PHF8 overexpression affected apoptosis. Cells were also transfected with the empty vector pFLAG-CMV as a control. Again cells were stained with Annexin V FITC and PI and analyzed using flow cytometry to detect apoptotic cells. As expected, cells overexpressing PHF8 were significantly less apoptotic compared to cells transfected with empty vector pFLAG-CMV (Figure 3.6). There was

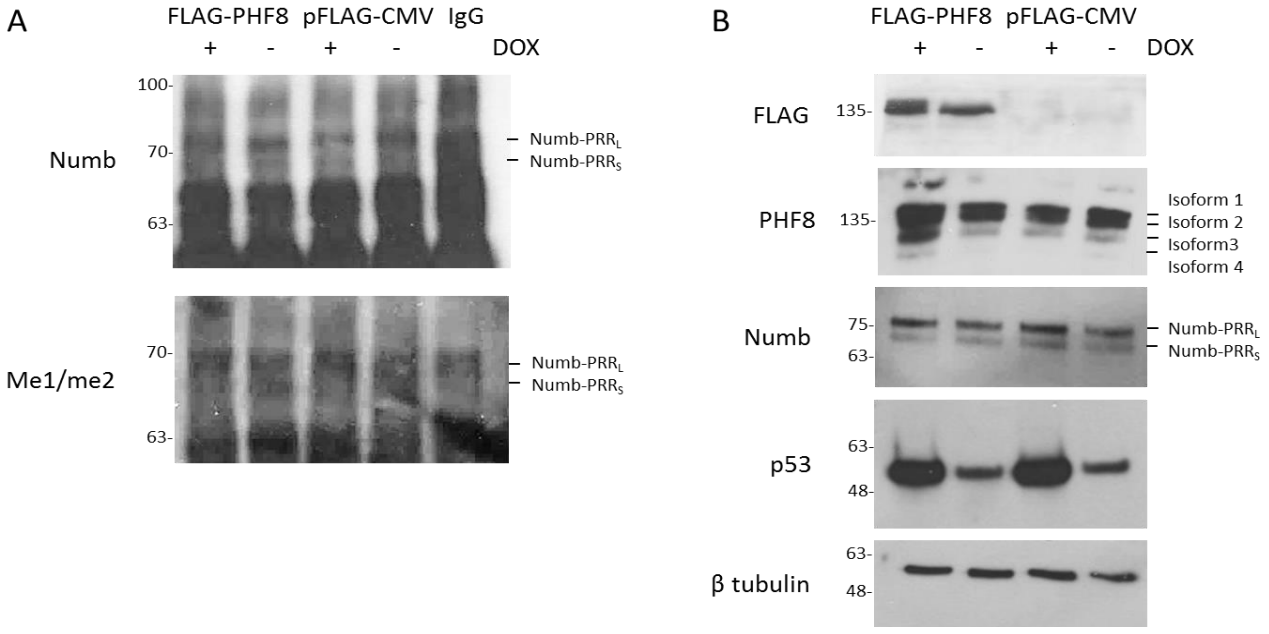

Figure 3.4: PHF8 does not demethylate Numb. HeLa cells were transfected with FLAG-PHF8 or pFLAG-CMV and treated with 1.0μM doxorubicin for 18 hours or left untreated. Cells were lysed and endogenous Numb was immunoprecipitated with anti-Numb antibody. The immunoprecipitate (A) and cell lysate (B) were run on 8% Bis-Tris SDS-PAGE and analyzed by western blot. Immunoprecipitate blots were blotted with anti-Numb and a pan-methylation antibody (A). Lysate blots were blotted with anti-FLAG, anti-PHF8, anti-Numb, anti-p53 and anti-β-tubulin (B).

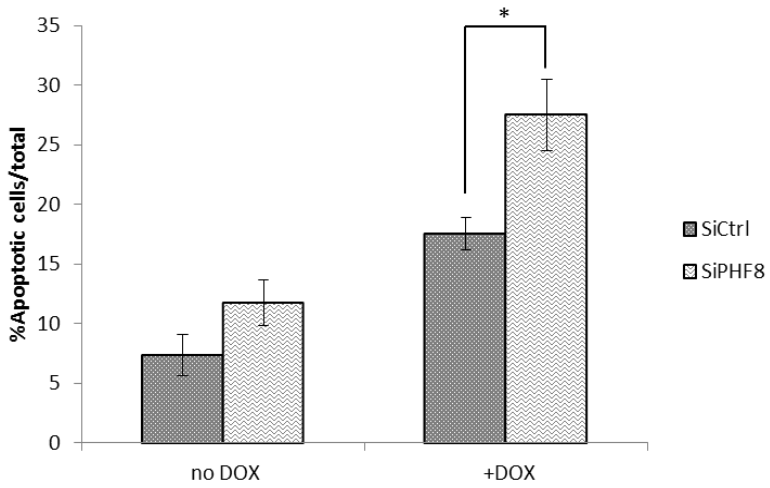

Figure 3.5: Cells transfected with siRNA against PHF8 undergo more apoptosis when treated with doxorubicin. HeLa cells were transfected with either siRNA against PHF8 or a scrambled control siRNA. Cells were treated with 1.0μM doxorubicin for 18 hours or left untreated. Annexin V FITC and propidium iodide were used to select for the apoptotic cells within the population. Apoptotic cells were identified using flow cytometry analysis. Data presented is the mean ±SEM of five biological repeats. *- indicates significant difference from the corresponding control ($p<0.025$).

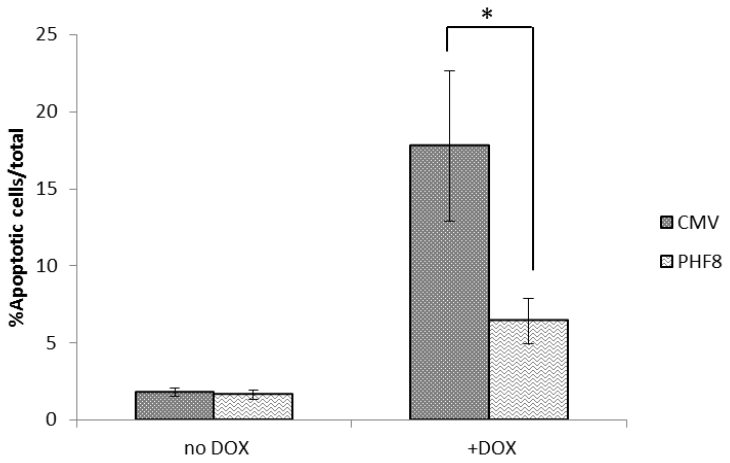

Figure 3.6: Cells overexpressing PHF8 undergo similar apoptosis as control cells when treated with doxorubicin. HeLa cells were transfected with either FLAG-PHF8 or pFLAG-CMV. Cells were treated with 1.0μM doxorubicin for 18 hours or left untreated. Annexin V FITC and PI were used to select for the apoptotic cells within the population. Apoptotic cells were identified using flow cytometry analysis. Data presented is the mean ±SEM of six biological repeats. *- indicates significant difference from the corresponding control ($p<0.025$).

no significant difference in apoptosis between untreated PHF8 overexpressing cells compared to untreated control cells.

3.5 PHF8 expression down regulates apoptotic genes

To further investigate the anti-apoptotic effect of PHF8, qRT-PCR was used to observe the effect of PHF8 activity on the expression of apoptotic genes that are involved in p53-mediated apoptosis. HeLa cells with PHF8 knocked down using siRNA or transfected with a scrambled control siRNA, were treated with 1.0 µM doxorubicin for 18 hours or left untreated prior to RNA extraction. The observed mRNA expression levels were normalized to the mRNA levels of the ribosomal protein Rpl13. As shown in figure 3.7 A, PHF8 mRNA levels were significantly reduced in knockdown cells confirming that PHF8 was successfully knocked down in these cells. The mRNA expression levels of p53 (*TP53*), Caspase3 (*CASP3*) and BAX (*BAX*) were all significantly up-regulated in doxorubicin treated PHF8 knockdown cells (Figure 3.7 B, C and D). Total p53 mRNA levels were significantly up-regulated in both doxorubicin treated and untreated cells when PHF8 was knocked down (Figure 3.7 B). Interestingly, no significant effect was seen on the mRNA levels of PUMA in either treated or untreated cells (Figure 3.7 E).

The same qRT-PCR experiments were repeated in cells overexpressing PHF8. HeLa cells were transfected with pFLAG-PHF8-CMV or pFLAG-CMV empty vector. The transfected cells were treated with 1.0 µM doxorubicin or left untreated prior to mRNA extraction. HeLa cells transfected with FLAG-PHF8 showed significantly higher levels of PHF8 mRNA when induced by doxorubicin compared to cells transfected with pFLAG-CMV (Figure 3.8 A). In cells overexpressing PHF8, the mRNA expression levels of p53, Caspase3 and BAX decreased significantly compared to cells transfected with the empty control vector, when cells were treated with doxorubicin (Figure 3.8 B, C and D).

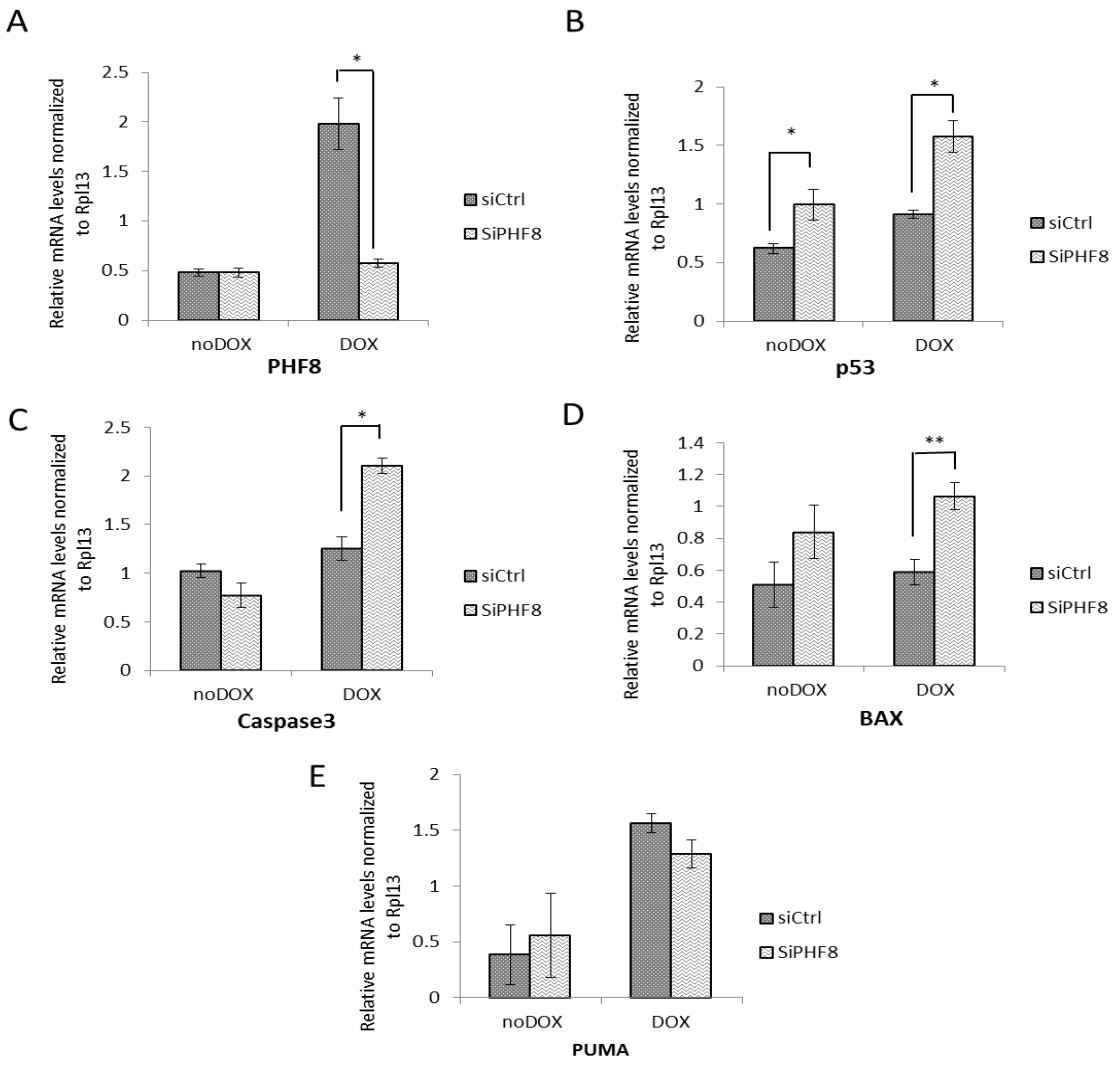

Figure 3.7: Transcript expression of apoptosis genes when PHF8 is knocked down. HeLa cells were transfected with siRNA against PHF8 (siPHF8) or scrambled siRNA (siCtrl). Total mRNA was extracted using TRIzol from the siRNA transfected cells treated with 1.0μM doxorubicin for 18 hours or from untreated cells. The mRNA was reverse transcribed into cDNA. Primers targeting the apoptotic genes *PHF8* (A), *TP53* (B), *CASP3* (C), *BAX* (D) and *PUMA* (E) were used to analyze levels of mRNA with qRT-PCR. Observed mRNA values were normalized to Rpl13. Data presented is the mean ±SEM of five biological repeats. *- indicates significant difference from the corresponding control ($p<0.025$). **- indicates significant difference from the corresponding control ($p<0.1$).

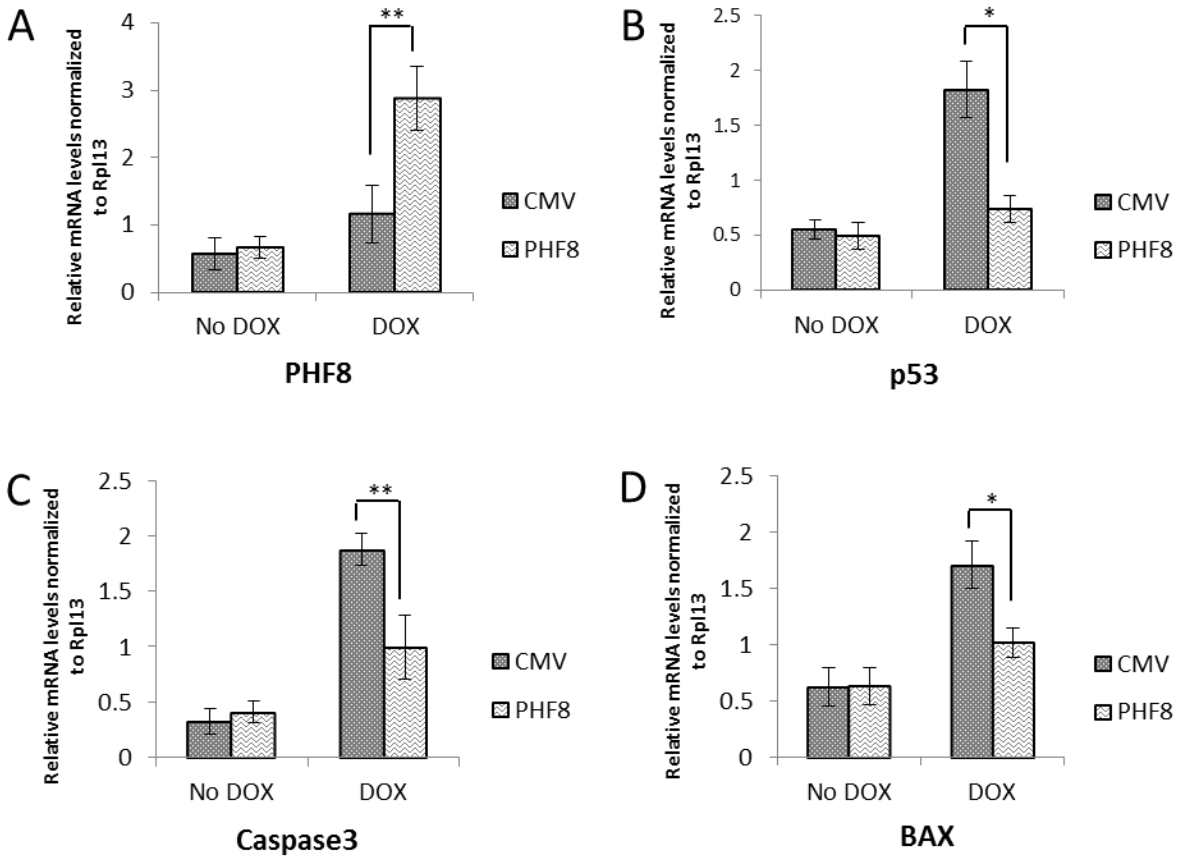

Figure 3.8: Transcript expression of apoptosis genes with PHF8 overexpressed. Total mRNA was extracted using TRIzol, from HeLa cells treated with 1.0μM doxorubicin for 18 hours or from untreated cells. The mRNA was reverse transcribed into cDNA and primers targeting the apoptotic genes *PHF8* (A), *TP53* (B), *CASP3* (C) and *BAX* (D) were used to analyze levels of mRNA with qPCR. The observed mRNA values were normalized to Rpl13 mRNA. Data presented is the mean ±SEM of five biological repeats. *- indicates significant difference from the corresponding control ($p<0.05$). **- indicates significant difference from the corresponding control ($p<0.1$).

3.6 PHF8 overexpression reduces p53 protein level

Since p53 is such an important protein, we found it interesting that PHF8 expression appeared to regulate the mRNA expression level of p53. To further confirm the down regulation of p53 expression by PHF8, SDS-PAGE and western blot analysis were used to observe the effect of PHF8 on p53 protein expression. pFLAG-PHF8-CMV or pFLAG-CMV plasmids were transfected into HeLa cells and the effects of PHF8 overexpression on p53 were observed. The protein expression level of p53 was decreased in cells overexpressing PHF8 with or without doxorubicin treatment compared to cells transfected with empty vector pFLAG-CMV (Figure 3.9 C). The levels of PHF8 and FLAG were also observed using anti-PHF8 and anti-FLAG antibodies respectively (Figure 3.9 A, B). To ensure equal loading, the levels of the housekeeping protein β-tubulin was also observed (Figure 3.9 D).

3.7 PHF8 binds to the promoters of the p53 and Caspase3 genes

Since we saw an effect of PHF8 overexpression and knockdown on the mRNA expression levels of p53, Caspase3 and BAX, we wondered in PHF8 was directly regulating their transcription. To investigate this chromatin immunoprecipitation (ChIP) was done to observe PHF8 binding to the promoters of the *TP53*, *CASP3* and *BAX* genes. HeLa cells were transfected with FLAG-PHF8 or pFLAG-CMV and treated with or without doxorubicin. Antibodies against either FLAG or RNA polymerase II (PolII) were used to immunoprecipitate PHF8 and PolII with their bound DNA. PolII was used as a positive control since it should be found at all active promoters. PolII was found to bind the promoter of GAPDH (Figure 3.10 E), whereas PHF8 only bound slightly and not significantly to the GAPDH promoter compared to the empty vector and IgG controls (Figure 3.10 A). Both PHF8 and PolII bound the *TP53* promoter significantly compared to the pFLAG-CMV and IgG controls (Figure 3.10 B and E), however there was no significant difference between doxorubicin treated and untreated cells (Figure 3.10 B). PHF8 bound the *TP53* promoter significantly more than that of *GAPDH* (Figure 3.10 A and B). PHF8 did not bind to the *BAX* promoter to the same extent as *TP53* or *CASP3* (3.10 D).

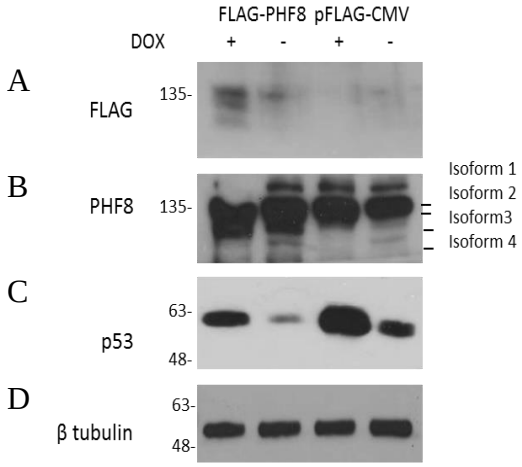

Figure 3.9: PHF8 overexpression reduces p53 protein levels. pFLAG-PHF8-CMV or pFLAG-CMV was transiently transfected into HeLa cells. Cells were either untreated or treated with 1.0μM doxorubicin for 18 hours. The cells were lysed and whole cell lysates were run on 8% Bis-Tris SDS-PAGE and analyzed by western blot. Blots were analyzed using anti-FLAG (A), anti-PHF8 (B), anti-p53 (C) and anti-βtubulin (D).

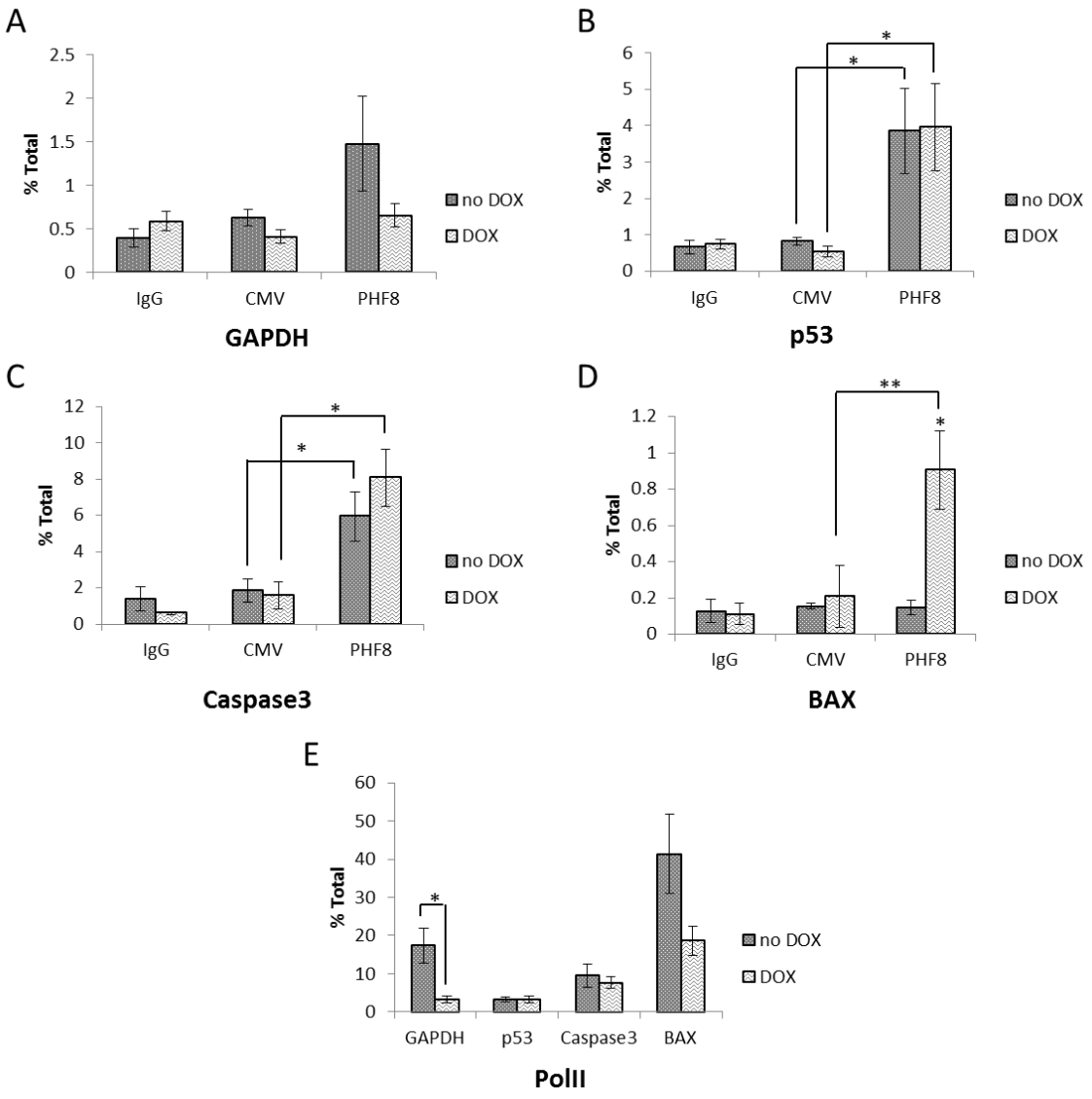

Figure 3.10: PHF8 binds the promoter of p53 and Caspase3 but not BAX. Cells over expressing PHF8 or an empty vector control (CMV) were fixed with formaldehyde to crosslink protein to their bound DNA. PHF8, PolII (E) and IgG were immunoprecipitated along with their bound DNA fragments. DNA was purified and *GAPDH* (A), *TP53* (B), *CASP3* (C) and *BAX* (D) genes were amplified using qRT-PCR. Values were normalized to input DNA. Data presented is the mean ±SEM of four biological repeats. *- indicates significant difference from the corresponding empty vector (CMV) and/or no doxorubicin control ($p<0.05$). **- indicates significant difference from the corresponding empty vector (CMV) control ($p<0.1$).

Since PHF8 appeared to be directly regulating p53 and Caspase3 transcription we then wanted to determine whether or not this regulation was through PHF8 demethylation of methylated H3K27. HeLa cells were transfected with siRNA to knock down PHF8 or scrambled control siRNA. The cells were treated with doxorubicin or left untreated. Anti-H3K27me3 was used to immunoprecipitated methylated H3K27 from the samples and qRT-PCR analysis was used to analyze the methylation status of H3K27 at the promoters of *TP53*, *CASP3* and *BAX*. As shown in Figure 3-11 B, cells with PHF8 knocked down and treated with doxorubicin had a significantly higher level of methylated H3K27 on the *TP53* promoter than the control siRNA cells. The untreated cells with PHF8 knocked down also showed significantly more methylated H3K27 than untreated control cells (Figure 3.11 B). Doxorubicin treated PHF8 knock down cells had more H3K27 methylation of the *CASP3* gene compared to cells transfected with scrambled siRNA (Figure 3.11 C). *GAPDH* H3K27 methylation levels were not significantly different between PHF8 knockdown cells and the control cells, with the exception of the significantly lower levels of H3K27 methylation in untreated control siRNA cells (Figure 3.11 A).

The same ChIP experiment was repeated with PHF8 overexpressed in HeLa cells transiently transfected with pFLAG-PHF8-CMV or transfected with the empty vector pFLAG-CMV. The cells were either treated with doxorubicin or left untreated and prepared for ChIP the same as above. Again anti-H3K27me3 was used to immunoprecipitate methylated H3K27. Cells with PHF8 overexpressed and treated with doxorubicin had a significantly lower level of methylated H3K27 on the *TP53* promoter than untreated PHF8 overexpressing cells (Figure 3.11 B). *CASP3* also displayed significantly lower levels of methylated H3K27 when cells were overexpressing PHF8 and treated with doxorubicin compared to the untreated PHF8 cells and vector control cells (Figure 3.11 C). Significantly higher levels of *GAPDH* H3K27 methylation was observed in control cells compared to PHF8 overexpressing cells (Figure 3.11 A). H3K27 methylation of the GAPDH gene was also significantly lower in cells treated with doxorubicin than the same cells untreated (Figure 3.11 A).

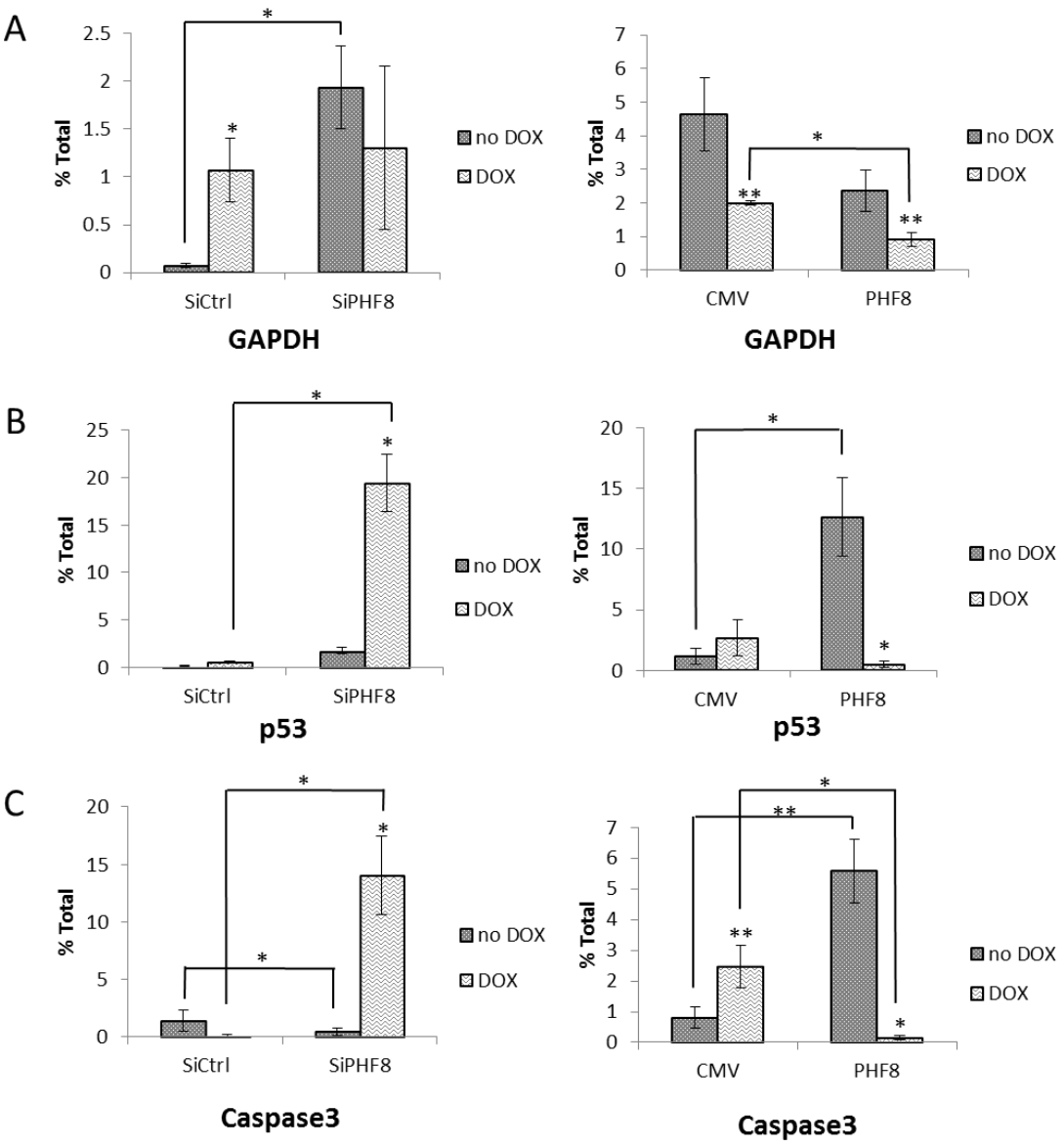

Figure 3.11: H3K27 methylation of GAPDH, p53 and Caspase3 genes. Cells over expressing PHF8 and PHF8 knockdown cells were fixed with formaldehyde to crosslink protein to their bound DNA. Anti-H3K27me3 was used to immunoprecipitate DNA fragments bound to methylated H3K27. DNA was purified and *GAPDH* (A), *TP53* (B) and *CASP3* (C) promoter DNA was amplified using qRT-PCR. Values were normalized to input DNA. Data presented is the mean ±SEM of four biological repeats. *- indicates significant difference from the corresponding SiRNA, empty vector (CMV) or no doxorubicin control ($p<0.05$). **- indicates significant difference from the corresponding empty vector (CMV) or no doxorubicin control ($p<0.1$).

Chapter 4

4 Discussion

The lysine demethylase PHF8 is a relatively recently discovered protein (Laumonnier *et al*., 2005). It was originally believed that methylation was a static modification until the identification of the first demethylase LSD1, which led to the realization that it is in fact a dynamic process (Shi *et al*., 2004). PHF8 is a lysine demethylase known to target H3K9me/me2, H3K27me2 (Yokoyama *et al*., 2010) and H4K20me (Liu *et al*., 2010). The majority of studies done on PHF8 have been on characterizing the role of PHF8 in X-linked mental retardation as well as its structure. More recently PHF8 has been identified as an oncogene (Björkman *et al*., 2012). The PHF8 protein has been found to have involvement in cell migration, proliferation and cycle progression (Asensio-Juan *et al*., 2012; Björkman *et al*., 2012; Sun *et al*., 2013; Liu *et al*., 2010). These functions of PHF8 have proven to play a role in the progression and pathogenicity of both prostate cancer and esophageal squamous cell carcinoma (Björkman *et al*., 2012; Sun *et al*., 2013). The anti-apoptotic effect of PHF8 has also been previously identified to add to its oncogenic function (Björkman *et al*., 2012; Sun *et al*., 2013), however until now no one had investigated the mechanism of how PHF8 affects apoptosis in any detail.

4.1 PHF8 is up-regulated during apoptosis but does not demethylate Numb

PHF8, among other demethylases, was identified as a possible Numb demethylase due to its ability to demethylate the histone lysine residues H3K27me/me2 (Yokoyama *et al*., 2010) and H4K20me (Liu *et al*., 2010). These two methylated histone residues share similar surrounding sequences to those of the methylated lysines of Numb (K158 and K163) (Dhami *et al*., 2013) (Table 3.1). Quantitative RT-PCR and western blot analysis revealed elevated PHF8 levels when apoptosis was induced by doxorubicin in both HeLa and U2OS cells (Figures 3.2 and 3.3), which was not seen for any other tested demethylase (Figure 3.1). Since other pro-apoptotic genes have been found to be elevated

during apoptosis (i.e. PUMA) (Dhami *et al*., 2013), we initially believed this meant that PHF8 has a pro-apoptotic function during apoptosis. We suspected that the pro-apoptotic function of PHF8 might have been in demethylating Numb so that it is able to bind to and stabilize p53. The mRNA levels of SET8, the methyltransferase responsible for methylating Numb, decreased when apoptosis was induced by doxorubicin as shown previously (Dhami *et al*., 2013) (Figure 3.2). Since the methyltranferase expression decreases with doxorubicin treatment, we suspected that the Numb demethylase expression would increase with doxorubicin treatment, leading us to believe that PHF8 could be a possible Numb demethylase. Unfortunately, our western blot analysis of Numb immunoprecipitated from PHF8 overexpressing cells with and without doxorubicin treatment suggested that PHF8 was not involved in Numb demethylation (Figure 3.4). Even though PHF8 does not demethylate Numb and has not yet been identified to act on any non-histone proteins, it is still possible that PHF8 may target non-histone proteins.

Histone modifying proteins have been known to carry out many diverse functions. They can act on a number of different genes by modifying the histone tail residues at the promoters of their target genes (Shi and Whetstine, 2007). They also sometimes act on non-histone proteins, such as SET8 methylating both Numb (Dhami *et al*., 2013) and p53 (Shi *et al*., 2007). The expression level of a given histone modifying enzyme does not necessarily change during a certain cellular process that it is or is not involved in. Therefore it is possible that a lysine demethylase whose mRNA expression level does not change significantly during apoptosis, such as KDM6A (Figure 3.1), may be responsible for Numb demethylation or possibly play some other role in apoptosis. Further investigation into which demethylase is responsible for demethylating Numb is still required. Identification of the Numb demethylase could potentially lead to the identification of the demethylase responsible for demethylating p53 K382, which shares sequence similarity and the same methyltransferase as Numb K158 and K163 (Dhami *et al*., 2013).

When observing PHF8 protein levels with doxorubicin treatment, we did not see an increase in PHF8 levels at the 6 hour time point (Figure 3.3). In U2OS cells there

appeared to be a decrease in PHF8 expression (Figure 3.3). Doxorubicin induces apoptosis through intercalation of the chemical into the DNA, causing excessive DNA damage (Yang *et al*., 2014). At the 6 hour time point it is possible that the cells are going through the DNA damage response and have not yet entered apoptosis. Therefore since we do not see an increase in PHF8 until the 18 hour time point (Figure 3.3), it is unlikely that PHF8 plays a role in the DNA damage response.

4.2 PHF8 promotes cell survival

Further study into PHF8's effect on apoptosis suggested an anti-apoptotic effect, contrary to our originally hypothesis that PHF8 was a pro-apoptotic protein. Flow cytometry analysis of PHF8 knockdown (Figure 3.5) and PHF8 overexpressing cells (Figure 3.6) demonstrated an anti-apoptotic effect on cells. PHF8 knockdown has previously been found to cause an increase in apoptosis (Björkman *et al*., 2012; Sun *et al*., 2013), however there was no further investigation into the mechanism behind this anti-apoptotic effect.

We decided to explore how PHF8 is negatively affecting p53-mediated apoptotic signaling in cells treated with doxorubicin. We found that PHF8 acts, at least in part, by down regulating genes required for apoptosis. Our qPCR analysis showed that PHF8 down-regulates p53, Caspase3 and BAX (Figures 3.7 and 3.8). BAX is a target gene of p53 (Miyashita *et al*., 1994), so it is likely that the effect seen on BAX expression is due to the down regulation of p53 by PHF8. PUMA is also an identified p53 target gene for p53-mediated apoptosis (Nakano and Vousden, 2001). We expected PHF8 to have a negative effect on PUMA mRNA expression since p53 is down regulated by PHF8; however we found that PUMA mRNA expression was not significantly affected by PHF8 (Figure 3.7). It has been suggested that PUMA up-regulation can occur in the absence of p53 (Luo *et al*., 2005; Dhami *et al*., 2013), therefore it is possible that we do not see an effect of PHF8 because PUMA is being regulated by a p53 independent mechanism. It would be interesting to observe the effects of PHF8 on other pro-apoptotic genes including other p53 target genes, such as Noxa another apoptotic protein. It would also be

of interest to observe the possible effects of PHF8 on anti-apoptotic genes. Since PHF8 is thought to promote transcription (Feng *et al*., 2010; Liu *et al*., 2010), it is possible PHF8 could be promoting transcription of anti-apoptotic genes to suppress apoptosis.

The negative effect of PHF8 on p53 expression was also observed at the protein level (Figure 3.9). As observed with qPCR, western blot analysis revealed that both the untreated and doxorubicin treated cell lysates experienced a decrease in p53 protein expression (Figure 3.9). The protein levels of the other apoptotic proteins were not analyzed due to limitations of reagent availability. The protein levels should be analyzed in the future to confirm the effect seen by qPCR. We would expect to see a decrease in protein expression of BAX and Caspase3 as well, at least when the cells are treated with doxorubicin. Since the expression levels of p53 was decreased at both the mRNA (Figure 3.8) and protein level (Figure 3.9) when PHF8 is overexpressed, we can conclude that PHF8 is affecting p53 at a transcriptional level, rather than post-translationally.

Histone modifying proteins typically bind to the gene promoters of the genes they are regulating. Chromatin immunoprecipitation revealed that PHF8 directly binds to the promoter of *TP53* and *CASP3*, but less significantly to that of *BAX* with PHF8 binding less than 1% of the total DNA (Figure 3.10). This further confirms that PHF8 is directly regulating the transcription of *TP53* and *CASP3*. As mentioned above, the negative effect seen on BAX mRNA level is likely a result of the inhibition of p53 transcription by PHF8 (Figures 3.7 and 3.8). However PHF8 has been shown to bind to PolII (Fortschegger *et al*., 2010), therefore it is possible that the localization seen at the promoters of *TP53*, *CASP3* and *GAPDH* could be due solely to this binding.

Since PHF8 demethylates H3K27me2 (Yokoyama *et al*., 2010), we decided to investigate if PHF8 is regulating the transcription of the affected apoptosis genes through demethylation of H3K27me2. A significant increase in H3K27 methylation was seen at both the *TP53* and *CASP3* promoters, when PHF8 was knocked down (Figure 3.11). Interestingly, when PHF8 is overexpressed H3K27 methylation at the *TP53* and *CASP3* promoters is significantly increased when untreated and significantly decreased when treated with doxorubicin, compare to empty vector control cells (Figure 3.11 B and C).

These findings suggest that PHF8 is regulating the promoters of *TP53* and *CASP3* through demethylation of methylated H3K27. Therefore, although PHF8 may be binding to PolII helping localize it to the genes of interest, PHF8 is also directly regulating these genes.

Methylated H3K27 has been described as a transcriptionally repressive mark (Vakoc *et al*., 2006). Therefore the results shown in this study appear to conflict with previously published literature. In the qPCR analysis, PHF8 appeared to have a suppressive effect on p53 and Caspase3 expression (Figures 3.7 and 3.8). However, the ChIP experiments reveal that PHF8 is demethylating H3K27me2, therefore removing a transcriptionally repressive mark (Figure 3.11). The ChIP data would suggest a transcriptionally activating activity of PHF8 whereas the qPCR data suggest a repressive function. There is likely more going on at these promoters that has yet to be identified, including a wide number of other histone tail modifications. PHF8 is also responsible for demethylating H3K9me/me2 (Yokoyama *et al*., 2010) and H4K20me (Liu *et al*., 2010). Therefore these ChIP experiments need to be repeated to observe the effect of PHF8 on these histone modifications at the *TP53* and *CASP3* promoters as well. The results may help us to better understand the mechanism of PHF8 transcriptional inhibition. It is possible that the demethylation of H3K27me2 is required for the recruitment of a repressive transcription factor. Another possibility could be that PHF8, although demethylating H3K27me2 may also be demethylating a transcriptionally activating transcription factor or histone modifying protein, thereby inhibiting the transcriptionally activating function. PHF8 has been found to interact with the transcription factors E2F transcription factor 1 (E2F1) and host cell factor C1 (HCF-1) as well as the methyltransferase SET1 (Liu *et al*., 2010), all of whose activity PHF8 could be affecting.

The transcription factor E2F1 has been found to activate p53 transcription in HeLa cells (Massip *et al*., 2013). Since PHF8 has been found to bind E2F1 (Liu *et al*., 2010), it is possible that E2F1 and PHF8 are interacting at the p53 promoter. These two previously published findings support our results that identify PHF8 binding to the promoter of p53 and regulation of p53 transcription. E2F1 is also known to up-regulate pro-apoptotic genes in response to genotoxic stress inducing apoptosis (Wu *et al*., 2009). Methylation

of lysing 158 of E2F1 by SET9 can increase apoptosis, whereas demethylation of this site by LSD1 decreases apoptosis (Xie *et al*., 2011). PHF8 may be involved in a similar mechanism to down regulate p53 and Caspase3 expression.

4.3 PHF8 regulation of p53

The p53 protein is known to be largely regulated at the post-translational level, since p53 is continuously being synthesized (Kubbutat *et al*., 1997). A lot less is known about p53's transcriptional regulation. Recently a number of proteins have been found to activate p53 transcription during DNA damage response and apoptosis. For example HoxA5 and Pitx1 have both been found to up-regulate transcription of the p53 gene to promote apoptosis (Raman *et al*., 2000; Liu and Lobie, 2007), whereas the proto-oncogene BCL6 is an example of a protein that inhibits p53 transcription (Phan and Ia-Favera, 2004). It is possible that PHF8 may be affecting p53 transcription by regulating one of these transcription factors through demethylation, either activating BCL6 or inhibiting HoxA5 or Pitx1.

We found that PHF8 is regulating the transcription of p53 (Figures 3.7 and 3.8); however it may also be directly affecting the p53 protein as well. The p53 protein is known to be methylated on a number of lysine residues, many of which the methyltransferases and demethylases responsible are unknown (Meek and Anderson, 2009). Lysine residue 382 of p53 has been found to have sequence similarities to H4K20 (Dhami *et al*., 2013), a target histone tail lysine of PHF8 (Liu *et al*., 2010). The methyltransferase SET8 is known to methylate p53K382 (Shi *et al*., 2007), however the demethylase responsible for its demethylation is unknown. It is possible that PHF8 could be demethylating p53K382.

Since PHF8 is known to promote cell cycle progression it is possible that PHF8 is inhibiting p53 during the cell cycle as well. The effect may be seen more in cancer cells which have elevated levels of PHF8, since we did not see much effect of PHF8 without doxorubicin treatment. The known role of PHF8 during the cell cycle is promoting the G2-M transition (Lim *et al*., 2013) and the G1-S transition (Liu *et al*, 2010), whereas p53

halts the cell cycle at the G1 to S phase transition when DNA damage is present (Kuerbitz *et al*., 1992). It is possible that PHF8 may be down regulating p53 when p53 is not required for cell cycle regulation.

4.4 PHF8 regulation of Caspase3

The lysine demethylase PHF8 plays a role in neuronal differentiation (Qiu *et al*., 2010). Mutations in the *PHF8* gene lead to X-linked mental retardation (XLMR) and cleft lip pallet (Laumonnier *et al*., 2005). Recently Caspase3 has also been found to be involved in neurogenesis (Tzeng *et al*., 2013). Since PHF8 regulates Caspase3 expression during p53-mediated apoptosis, it is possible that PHF8 may have an effect on the CASP3 gene in neuronal cells during neurogenesis. If PHF8 is somehow regulating Caspase3, this may be one way that inactivating mutations of PHF8 leads to XLMR. Further studies are needed to investigate this possibility.

4.5 PHF8 as an oncogene

The down regulation of p53 by PHF8 supports the previously identified oncogenic effects of PHF8. The p53 protein plays a very important tumor suppressor role for cells and tissues. It blocks cell cycle progression when the cell is experiencing some sort of stress or there is DNA damage detected that needs repairing (Kuerbitz *et al*., 1992; Read and Strachan, 1999). Inhibition of the cell cycle by p53 stops the mutation in the DNA from being replicated and passed on to daughter cells which could potentially lead to cancer (Read and Strachan, 1999). The p53 protein is also involved in the DNA damage response and DNA repair itself (Meek, 2009). Finally when the DNA damage is too great to be repaired p53 protects the tissue again by signaling for the cell to undergo apoptosis (Meek, 2009). We have found that PHF8 inhibits p53 from inducing apoptosis (Figures 3.6 and 3.8) and although not yet determined, it is possible that PHF8 may be inhibiting the transcription of p53 during the cell cycle as well. The suppressive effect that PHF8 has on p53 could lead to cancer if not properly regulated.

It is well known that cancer is the additive result of a number of mutations that lead to the hallmarks of cancer (Hanahan and Weinberg, 2000). Therefore it would be unfair to say that PHF8 mutations can cause cancer but it could have an oncogenic effect. It is also well known that p53 is a highly regulated protein that is acted on by a large number of proteins (Meek and Anderson, 2009). Therefore the effect PHF8 has as a single protein might not be that significant *in vivo*. However, since PHF8 is regulating the transcription of p53 directly rather than post-translationally (Figures 3.7, 3.8 and 3.10) like the majority of other p53 regulating proteins (Meek and Anderson, 2009), PHF8 could have a more significant effect on p53. PHF8 also down regulates Caspase3 expression (Figures 3.7 and 3.8) which is an important protein for apoptosis. Therefore the significant down-regulation of apoptosis by PHF8 (Figures 3.5 and 3.6) does suggest that it can cause one of the hallmarks of cancer; evasion of apoptotic signaling (Hanahan and Weinberg, 2000).

There is a lot that remains to be learned about PHF8's oncogenic functions. So far we have only observed the effects PHF8 has on the cell, such as cell cycle progression/ cell proliferation, cell migration and apoptosis (Bjorkman *et al*., 2012; Sun *et al*., 2013). A lot of work is still required to determine the underlying mechanisms causing these oncogenic effects. Once we can better understand this protein, we can attempt to develop better therapies to target PHF8 in cancer patients with PHF8 overexpression, for custom designed treatment programs.

4.6 Therapeutic potential of PHF8

Cancer treatments typically involve the use of radiation therapy and/or chemotherapy. The main goal of these treatments is to kill the cancer cells; unfortunately these treatments are not always successful. Sometimes cancer cells have the ability to evade apoptosis, which can lead to failed treatments and relapse. Due to its oncogenic anti-apoptotic effects, PHF8 would make a good target for cancer therapy. Used in combination with other treatments, a drug designed to inhibit PHF8 could potentially be used to target the cells that are evading apoptosis, making them more susceptible to cell

death. There has already been work done to create small peptide inhibitors to block the function of lysine methyltransferases and lysine demethylases (Rose *et al*., 2010). Both the PHD domain and the JmjC domain could be targeted on PHF8, however one study found that mutating the PHD domain did not inhibit its demethylase activity (Yue *et al*., 2010). Therefore, targeting the catalytic JmjC domain would be the best target to inhibit PHF8 activity.

PHF8 and other JmjC containing demethylases require both iron Fe(II) and α-ketogluterate as co-factors for the catalysis of the demethylation reaction. These demethylases can therefore be inhibited by metal chelators such as desferoxamine (Barman-Aksözen *et al*., 2013). α-ketogluterate mimics have also proven to inhibit JmjC domain containing demethylases, such as N-oxalyglycine (Hamanda *et al*., 2009) and pyridine-2,4-dicarboxylic acid (Mackeen *et al*., 2010; Loenarz et al., 2010). Unfortunately, chemicals which target co-factor binding to these demethylases are not going to be specific to inhibit a specific JmjC demethylase. Small molecule inhibitors have also been designed to inhibit JmjC demethylases. Luo *et al*., (2011) has identified a small molecule which mimics a methylated lysine residue connected to an α-ketogluterate mimic that is able to bind to and inhibit the JmjC containing demethylase KDM6A. Another small molecule, 2-4(4-methylphenyl)-1,2-benzisothiazol-3(2H)-one, another metal ion chealator, has been identified to inhibit the JmjC demethylase Jumonji AT-rich interactive domain 1B (JARID1B)(Sayegh *et al*., 2013). Given the observed oncogenic activity of PHF8 a small molecule designed to specifically inhibit PHF8 would prove beneficial.

4.7 Future directions

This study has only started to give us insight into PHF8's anti-apoptotic effects. There are many questions that remain to be answered. First, the still unanswered question of which lysine demethylase is demethylating Numb during the induction of apoptosis. Further investigation into the other suspected demethylases could lead to an answer to this question. Next, the biggest question that arises from the findings of this study is how

PHF8 is negatively regulating the transcription of p53 and Caspase3. What proteins are binding along with PHF8 at the promoters of these genes? How might PHF8 be affecting the activity of these proteins? Or how might these proteins affect PHF8 activity? PHF8 could also be regulating a number of other proteins involved in apoptosis. Does PHF8 bind to the promoters of other pro-apoptotic genes negatively regulating their transcription? Is PHF8 up-regulating any anti-apoptotic proteins during apoptosis? As mentioned previously, there is also the possibility that PHF8 could be regulating p53 or Caspase3 transcription during other cellular processes, such as whether or not there is any effect of PHF8 on p53 during the cell cycle or if PHF8 affects Caspase3 during neurogenesis. Future research to answer these questions will give us a better understanding of PHF8's pro-apoptotic activities as well as further insight into the overall oncogenic effect of PHF8.

4.8 Conclusions

In summary, PHF8 has a negative regulatory effect on p53-mediated apoptosis, even though its expression levels increase during apoptosis. We found that PHF8 does not demethylate Numb as we had initially suspected, which would have been a pro-apoptotic effect. Instead, PHF8's anti-apoptotic effect is at least in part due to its down-regulation of the pro-apoptotic genes *TP53*, *BAX* and *CASP3*. PHF8 directly binds to the promoters of *TP53* and *CASP3*, demethylating H3K27me2. The negative effect on BAX transcription was likely the result of an indirect effect of p53 down-regulation, since BAX is transactivated by p53. However, it is unlikely that the inhibition of *TP53* and *CASP3* transcription by PHF8 is simply the result of PHF8 affecting H3K27 methylation. H3K27 demethylation is typically thought to have an activating effect on transcription. Therefore we suspect other proteins could be involved in the observed transcriptional inhibition and that PHF8 possibly could be regulating them. The question of how PHF8 is affecting the methylation status of H3K9me/me2 and H4K20me also requires further investigation.

References

1. Abbas T, Shibata E, Park J, Jha S, Karnani N, Dutta A. (2010) CRL4(Cdt2) regulates cell proliferation and histone gene expression by targeting PR-Set7/Set8 for degradation. *Mol Cell. 40*, 9-21.
2. Abidi, F., Miano, M., Murray, J., Schwartz, C. (2007) A novel mutation in the PHF8 gene is associated with X-linked mental retardation with cleft lip/cleft palate. *Clin Genet. 72*, 19-22.
3. Acehan, D., Jiang, X., Morgan, D.G., Heuser, J.E., Wang, X. and Akey, C.W. (2002) Three-dimensional structure of the apoptosome: implications for assembly, procaspase-9 binding, and activation. Mol. Cell 9, 423–432.
4. Asensio-Juan, E., Gallego, C., Martínez-Balbás, M.A. (2012) The histone demethylase PHF8 is essential for cytoskeleton dynamics. *Nucleic Acids Res. 40*, 9429-9440.
5. Barman-Aksözen, J., Béguin, C., Dogar, A.M., Schneider-Yin, X., Minder, E.I. (2013) Iron availability modulates aberrant splicing of ferrochelatase through the iron- and 2-oxoglutarate dependent dioxygenase Jmjd6 and U2AF(65.). *Blood Cells Mol Dis. 51*, 151-161.
6. Bechtel, S., Rosenfelder, H., Duda, A., Schmidt, C.P., Ernst, U., Wellenreuther, R., Mehrle, A., Schuster, C., Bahr, A., Bloecker, H., Heubner, D., Hoerlein, A., Michel, G., Wedler, H., Koehrer, K., Ottenwaelder, B., Poustka, A., Wiemann, S., Schupp, I. (2007) The full-ORF clone resource of the German cDNA consortium. *BMC Genomics. 8*, 399.
7. Björkman, M., Östling, P., Härmä, V., Virtanen, J., Mpindi, J.P., Rantala, J., Mirtti, T., Vesterinen, T., Lundin, M., Sankila, A., Rannikko, A., Kaivanto, E., Kohonen, P., Kallioniemi, O., Nees, M. (2012) Systematic knockdown of epigenetic enzymes identifies a novel histone demethylase PHF8 overexpressed in prostate cancer with an impact on cell proliferation, migration and invasion. *Oncogene. 31*, 3444-3456.
8. Bork, P. and Margolis, B. (1995) A phosphotyrosine interaction domain. *Cell. 80*, 693-694.
9. Canman, C.E., Lim, D.S., Cimprich, K.A., Taya, Y., Tamai, K., Sakaguchi, K., Appella, E., Kastan, M.B., Siliciano, J.D. (1998) Activation of the ATM kinase by ionizing radiation and phosphorylation of p53. *Science. 281*, 1677-1679.
10. Chipuk, J.E., Kuwana, T., Bouchier-Hayes, L., Droin, N.M., Newmeyer, D.D., Schuler, M., Green, D.R. (2004) Direct activation of Bax by p53 mediates mitochondrial membrane permeabilization and apoptosis. *Science. 303*, 1010-1014.
11. Chuikov, S., Kurash, J.K., Wilson, J.R., Xiao, B., Justin, N., Ivanov, G.S., McKinney, K., Tempst, P., Prives, C., Gamblin, S.J., Barlev, N.A., Reinberg, D. (2004) Regulation of p53 activity through lysine methylation. *Nature. 432*, 353-360.
12. Crawford, L. (1983) The 53,000-dalton cellular protein and its role in transformation. *Int Rev Exp Pathol. 25*, 1–50.

13. Dhami, G.K., Liu, H., Galka, M., Voss, C., Wei, R., Muranko, K., Kaneko, T., Cregan, S.P., Li, L., Li, S.S. (2013) Dynamic methylation of Numb by Set8 regulates its binding to p53 and apoptosis. *Mol Cell. 50*, 565-76.
14. El-Deiry, W., Tokino, T., Velculescu, V. E., Levy, D. B., Parson, V. E., Trent, J. M. et al. (1993) WAF1, a potential mediator of p53 tumour suppression. *Cell. 75*, 817–825.
15. Elmore, S. (2007) Apoptosis: a review of programmed cell death. *Toxicol Pathol. 35*, 495-516.
16. Fadok, V.A., Bratton, D.L., Frasch, S.C., Warner, M.L., Henson, P.M. (1998) The role of phosphatidylserine in recognition of apoptotic cells by phagocytes. *Cell Death Differ. 5*, 551-562.
17. Feng, W., Yonezawa, M., Ye, J., Jenuwein, T., Grummt, I. (2010) PHF8 activates transcription of rRNA genes through H3K4me3 binding and H3K9me1/2 demethylation. *Nat Struct Mol Biol. 17*, 445-450.
18. Follis, A.V., Chipuk, J.E., Fisher, J.C., Yun, M.K., Grace, C.R., Nourse, A., Baran, K., Ou, L., Min, L., White, S.W., Green, D.R., Kriwacki, R.W.. (2013) PUMA binding induces partial unfolding within BCL-xL to disrupt p53 binding and promote apoptosis. *Nat Chem Biol. 9*, 163-168.
19. Fortschegger, K., de Graaf, P., Outchkourov, N.S., van Schaik, F.M., Timmers, H.T., Shiekhattar, R. (2010) PHF8 targets histone methylation and RNA polymerase II to activate transcription. *Mol Cell Biol. 30*, 3286-3298.
20. Fortschegger, K. and Shiekhattar, R. (2011) Plant homeodomain fingers form a helping hand for transcription. *Epigenetics. 6*, 4-8.
21. Garrido, C., Galluzzi, L., Brunet, M., Puig, P.E., Didelot, C., Kroemer, G. (2006) Mechanisms of cytochrome c release from mitochondria. *Cell Death Differ. 13*, 1423–1433.
22. Gotz, C. and Montenarh, M. (1995) p53 and its implication in apoptosis (review). *Int J Oncol. 6*, 1129-1135.
23. Gross, A., McDonnell, J.M., Korsmeyer, S.J. (1999) BCL-2 family members and the mitochondria in apoptosis. *Genes Dev. 13*, 1899–1911
24. Gulino, A., Di Marcotullio, L., Screpanti, I. (2010) The multiple functions of Numb. *Exp Cell Res. 316*, 900-906.
25. Hamada, S., Kim, T.D., Suzuki, T., Itoh, Y., Tsumoto, H., Nakagawa, H., Janknecht, R., Miyata, N. (2009) Synthesis and activity of N-oxalylglycine and its derivatives as Jumonji C-domain-containing histone lysine demethylase inhibitors. *Bioorg Med Chem Lett. 19*, 2852-2855.
26. Hanahan, D. and Weinberg, R.A. (2000) The hallmarks of cancer. *Cell. 100*, 57-70.
27. Haupt, Y., Maya, R., Kazaz, A., and Oren, M. (1997) MDM2 promotes the rapid degradation of p53. *Nature. 387*, 296 – 299.
28. Hong, S., Cho, Y. W., Yu, L. R., Yu, H., Veenstra, T. D., Ge, K. (2007) Identification of JmjC domain-containing UTX and JMJD3 as histone H3 lysine 27 demethylases. *Proc Natl Acad Sci USA. 104*, 18439–18444.
29. Horvitz, H. R. (1999) Genetic control of programmed cell death in the nematode Caenorhabditis elegans. *Cancer Res 59*, 1701s–1706s.

30. Huang, J., Perez-Burgos, L., Placek, B.J., Sengupta, R., Richter, M., Dorsey, J.A., Kubicek, S., Opravil, S., Jenuwein, T., Berger, S.L. (2006) Repression of p53 activity by Smyd2-mediated methylation. *Nature. 444*, 629-32.
31. Juven-Gershon, T., Shifman, O., Unger, T., Elkeles, A., Haupt, Y., Oren, M. (1998) The Mdm2 oncoprotein interacts with the cell fate regulator Numb. *Mol. Cell. Biol. 18*, 3974–3982.
32. Kikuno, R., Nagase, T., Ishikawa, K., Hirosawa, M., Miyajima, N., Tanaka, A., Kotani, H., Nomura, N., Ohara, O. (1999) Prediction of the coding sequences of unidentified human genes. XIV. The complete sequences of 100 new cDNA clones from brain which code for large proteins in vitro. *DNA Res. 6*:197-205.
33. Klose, R.J., Kallin, E.M. and Zhang, Y. (2006) JmjC-domain-containing proteins and histone demethylation. *Nat Rev Genet. 7*, 715-727.
34. Koivisto, A.M., Ala-Mello, S., Lemmelä, S., Komu, H.A., Rautio, J., Järvelä, I. (2007) Screening of mutations in the PHF8 gene and identification of a novel mutation in a Finnish family with XLMR and cleft lip/cleft palate. *Clin Genet. 72*, 145-149.
35. Kress, M., May, E., Cassingena, R., May, P. (1979) Simian virus 40-transformed cells express new species of proteins precipitable by anti-simian virus 40 tumor serum. *Virol J. 31*, 472–483.
36. Krishnan, S., Horowitz, S. and Trievel, R.C. (2011) Structure and function of histone H3 lysine 9methyltransferases and demethylases. *Chem Bio Chem. 12*, 254-263.
37. Kubbutat, M.H., Jones, S.N. and Vousden, K.H. (1997) Regulation of p53 stability by Mdm2. *Nature. 387*, 299-303.
38. Kuerbitz, S.J., Plunkett, B.S., Walsh, W.V., Kastan, M.B. (1992) Wild-type p53 is a cell cycle checkpoint determinant following irradiation. *Proc Natl Acad Sci USA. 89*, 7491–7495.
39. Kuwana, T., Bouchier-Hayes, L., Chipuk, J.E., Bonzon, C., Sullivan, B.A., Green, D.R., Newmeyer, D.D. (2005) BH3 domains of BH3-only proteins differentially regulate Bax-mediated mitochondrial membrane permeabilization both directly and indirectly. *Mol Cell. 17*, 525–535.
40. Lan, F., Bayliss, P.E., Rinn, J.L., Whetstine, J.R., Wang, J.K., Chen, S., Iwase, S., Alpatov, R., Issaeva, I., Canaani, E., Roberts, T.M., Chang, H.Y., Shi, Y. (2007) A histone H3 lysine 27 demethylase regulates animal posterior development. *Nature. 449*, 689-694.
41. Lane, D. P. and Crawford, L. V. (1979) T antigen is bound to a host protein in SV40-transformed cells. *Nature. 278*, 261–263.
42. Laumonnier, F., Holbert, S., Ronce, N., Faravelli, F., Lenzner, S., Schwartz, C.E., Lespinasse, J., Van Esch, H., Lacombe, D., Goizet, C., Phan-Dinh Tuy, F., van Bokhoven, H., Fryns, J.P., Chelly, J., Ropers, H.H., Moraine, C., Hamel, B.C., Briault, S. (2005) Mutations in PHF8 are associated with X linked mental retardation and cleft lip/cleft palate. *J Med Genet. 42*,780-786.
43. Levine, A. J. (1997) p53, the cellular gatekeeper for growth and division. *Cell. 88*, 323–331.
44. Li, S.C., Songyang, Z., Vincent, S.J., Zwahlen, C., Wiley, S., Cantley, L., Kay, L.E., Forman-Kay, J., Pawson, T. (1997) High-affinity binding of the Drosophila

Numb phosphotyrosine-binding domain to peptides containing a Gly-Pro-(p)Tyr motif. *Proc. Natl. Acad. Sci. USA. 94*, 7204−7209.

45. Li, S.C., Zwahlen, C., Vincent, S.J., McGlade, C.J., Kay, L.E., Pawson, T., Forman-Kay, J.D. (1998) Structure of a Numb PTB domain-peptide complex suggests a basis for diverse binding specificity. *Nat Struct Biol. 5*, 1075–1083.
46. Lim, H.J., Dimova, N.V., Tan, M.K., Sigoillot, F.D., King, R.W., Shi, Y. (2013) The G2/M regulator histone demethylase PHF8 is targeted for degradation by the anaphase-promoting complex containing CDC20. *Mol Cell Biol. 33*, 4166-4180.
47. Linzer, D.I. and Levine, A. J. (1979) Characterization of a 54K dalton cellular SV40 tumor antigen present in SV40-transformed cells and uninfected embryonal carcinoma cells. *Cell. 17*, 43–52.
48. Liu, W., Tanasa, B., Tyurina, O.V., Zhou, T.Y., Gassmann, R., Liu, W.T., Ohgi, K.A., Benner, C., Garcia-Bassets, I., Aggarwal, A.K., Desai, A., Dorrestein, P.C., Glass, C.K., Rosenfeld, M.G. (2010) PHF8 mediates histone H4 lysine 20 demethylation events involved in cell cycle progression. *Nature. 466*, 508-512.
49. Liu, D.X. and Lobie, P.E. (2007) Transcriptional activation of p53 by Pitx1. *Cell Death Differ. 14*, 1893-1907.
50. Locksley, R. M., Killeen, N., and Lenardo, M. J. (2001) The TNF and TNF receptor superfamilies: integrating mammalian biology. *Cell. 104*, 487–501.
51. Loenarz, C., Ge, W., Coleman, M.L., Rose, N.R., Cooper, C.D.O., Klose, R.J., Ratcliffe, P.J., Schofield, C.J. (2009) PHF8, a gene associated with cleft lip/palate and mental retardation, encodes for an Ne-dimethyl lysine demethylase. *Hum. Mol. Gen. 19*, 217-222.
52. Luo, X., He, Q., Huang, Y., Sheikh, M.S. (2005) Transcriptional up-regulation of PUMA modulates endoplasmic reticulum calcium pool depletion-induced apoptosis via Bax activation. *Cell Death Differ. 12*, 1310-1318.
53. Luo, X., Liu, Y., Kubicek, S., Myllyharju, J., Tumber, A., Ng, S., Che, K.H., Podoll, J., Heightman, T.D., Oppermann, U., Schreiber, S.L., Wang, X. (2011) A selective inhibitor and probe of the cellular functions of Jumonji C domain-containing histone demethylases. *J Am Chem Soc. 133,* 9451-9456.
54. Mackeen, M.M., Kramer, H.B., Chang, K.H., Coleman, M.L., Hopkinson, R.J., Schofield, C.J., Kessler, B.M. (2010) Small-molecule-based inhibition of histone demethylation in cells assessed by quantitative mass spectrometry. *J Proteome Res. 9*, 4082-4092.
55. Margueron, R., Trojer, P. and Reinberg, D. (2005) The key to development: interpreting the histone code? *Curr. Opin. Genet. Dev. 15*, 163-176.
56. Massip, A., Arcondéguy, T., Touriol, C., Basset, C., Prats, H., Lacazette, E. (2013) E2F1 activates p53 transcription through its distal site and participates in apoptosis induction in HPV-positive cells. *FEBS Lett. 587*, 3188-3194.
57. McGill M.A. and McGlade C.J. (2003) Mammalian numb proteins promote Notch1 receptor ubiquitination and degradation of the Notch1 intracellular domain. *J Biol Chem. 278*, 23196-23203.
58. Meek, D.W. (2009) Tumour suppression by p53: a role for the DNA damage response? *Nat Rev Cancer. 9*, 714-23.
59. Meek, D.W. and Anderson, C.W. (2009) Posttranslational Modification of p53: Cooperative Integrators of function. *Cold Spring Harb Perspect Biol*. 1, a000950.

60. Miyashita, T., Krajewski, S., Krajewska, M., Wang, H.G., Lin, H.K., Liebermann, D.A., Hoffman, B., Reed, J.C. (1994) Tumor suppressor p53 is a regulator of bcl-2 and bax gene expression in vitro and in vivo. *Oncogene. 9*, 1799-1805.
61. Nakano, K. and Vousden, K.H. (2001) PUMA, a novel proapoptotic gene, is induced by p53. *Mol Cell. 7*, 683-694.
62. Nishimura, T. and Kaibuchi, K. (2007) Numb controls integrin endocytosis for directional cell migration with aPKC and PAR-3. *Dev Cell. 13*, 15-28.
63. Nishioka, K., Rice, J. C., Sarma, K., Erdjument-Bromage, H., Werner, J., Wang, Y., Chuikov, S., Valenzuela, P., Tempst, P., Steward, R., Lis, J. T., Allis, C. D., Reinberg, D. (2002) PR-Set7 is a nucleosome-specific methyltransferase that modifies lysine 20 of histone H4 and is associated with silent chromatin. *Mol Cell. 9*, 1201-1213.
64. Ng, H.-H., Robert F., Young, R. A., Struhl, K. (2003) Targeted recruitment of Set1 histone methylase by elongating Pol II provides a localized mark and memory of recent transcriptional activity. *Mol. Cell. 11*, 709-719.
65. Oda, E., Ohki, R., Murasawa, H., Nemoto, J., Shibue, T., Yamashita, T., Tokino, T., Taniguchi, T., Tanaka, N. (2000) Noxa, a BH3-only member of the Bcl-2 family and candidate mediator of p53-induced apoptosis. *Science. 288*, 1053-1058.
66. Oltvai, Z.N., Milliman, C.L. and Korsmeyer, S.J. (1993) Bcl-2 heterodimerizes in vivo with a conserved homolog, Bax, that accelerates programmed cell death. *Cell. 74*, 609-619.
67. Ota, T., Suzuki, Y., Nishikawa, T., Otsuki, T., Sugiyama, T., Irie, R., Wakamatsu, A., Hayashi, K., Sato, H., Nagai, K., Kimura, K., Makita, H., Sekine, M., Obayashi, M., Nishi, T., Shibahara, T., Tanaka, T., Ishii, S., Sugano, S. (2004) Complete sequencing and characterization of 21, 243 full-length human cDNAs. *Nat Genet. 36*, 40-45.
68. Pha, R.T. and la-Favera, R. (2004) The BCL6 proto-oncogene suppresses p53 expression in germinalcentre B cells. *Nature. 432*, 635–639.
69. Qiu, J., Shi, G., Jia, Y., Li, J., Wu, M., Li, J., Dong, S., Wong, J. (2010) The X-linked mental retardation gene PHF8 is a histone demethylase involved in neuronal differentiation. *Cell Res. 20*, 908-918.
70. Raman, V., Martensen, S.A., Reisman, D., Evron, E., Odenwald, W.F., Jaffee, E., Marks, J., Sukumar, S. (2000) Compromised HOXA5 function can limit p53 expression in human breast tumours. *Nature. 405*, 974–978.
71. Rea, S., Eisenhaber, F., O'Carroll, D., Strahl, B.D., Sun, Z.-W., Schmid, M., Opravil, S., Mechtier, K., Ponting, C.P., Allis, C.D., and Jenuwein, T. (2000). Regulation of chromatin structure by site-specific histone H3 methyltransferases. *Nature. 406*, 593–599.
72. Renehan, A. G., Booth, C., and Potten, C. S. (2001) What is apoptosis, and why is it important? *Bmj. 322*, 1536–1538.
73. Riley, T., Sontag, E., Chen, P., Levine, A. (2008) Transcriptional control of human p53-regulated genes. *Nature Rev. Mol. Cell Biol. 9*, 402–412.
74. Roguev, A., Schaft, D., Shevchenko, A., Pijnappel, W.W., Wilm, M., Aasland, R., Stewart, A.F. (2001)The Saccharomyces cerevisiae Set1 complex includes an Ash2 homologue and methylates histone 3 lysine 4. *EMBO J. 20*, 7137–7148.

75. Rose, N.R., Woon, E.C., Kingham, G.L., King, O.N., Mecinović, J., Clifton, I.J., Ng, S.S., Talib-Hardy, J., Oppermann, U., McDonough, M.A., Schofield, C.J. (2010) Selective inhibitors of the JMJD2 histone demethylases: combined nondenaturing mass spectrometric screening and crystallographic approaches. *J Med Chem. 53*, 1810-1818.
76. Saito, S., Goodarzi, A.A., Higashimoto, Y., Noda, Y., Lees-Miller, S.P., Appella, E., Anderson, C.W. (2002) ATM mediates phosphorylation at multiple p53 sites, including Ser(46), in response to ionizing radiation. *J Biol Chem. 277*, 12491-12494.
77. Santolini, E., Puri, C., Salcini, A.E., Gagliani, M.C., Pelicci, P.G., Tacchetti, C., Di Fiore, P.P. (2000) Numb is an endocytic protein. *J Cell Biol. 151*, 1345-1352.
78. Sayegh, J., Cao, J., Zou, M.R., Morales, A., Blair, L.P., Norcia, M., Hoyer, D., Tackett, A.J., Merkel, J.S., Yan, Q. (2013) Identification of small molecule inhibitors of Jumonji AT-rich interactive domain 1B (JARID1B) histone demethylase by a sensitive high throughput screen. *J Biol Chem. 288*, 9408-9417.
79. Shi, X., Kachirskaia, I., Yamaguchi, H., West, L.E., Wen, H., Wang, E.W., Dutta, S., Appella, E., Gozani, O. (2007) Modulation of p53 function by SET8-mediated methylation at lysine 382. *Mol Cell. 27*, 636-46.
80. Shi, Y., Lan, F., Matson, C., Mulligan, P., Whetstine, J.R., Cole, P.A., Casero, R.A., and Shi, Y. (2004) Histone demethylation mediated by the nuclear amine oxidase homolog LSD1. *Cell. 119*, 941–953.
81. Shi, Y. and Whetstine, J.R. (2007) Dynamic regulation of histone lysine methylation by demethylases. *Mol Cell. 25*, 1-14.
82. Soussi, T. and Béroud, C. (2001) Assessing TP53 status in human tumours to evaluate clinical outcome. *Nature Reviews Cancer. 1*, 233–240.
83. Sun, X., Qiu, J.J., Zhu, S., Cao, B., Sun, L., Li, S., Li, P., Zhang, S., Dong, S. (2013) Oncogenic features of PHF8 histone demethylase in esophageal squamous cell carcinoma. *PLoS One. 8*:e77353.
84. Tang, Y., Zhao, W., Chen, Y., Zhao, Y., Gu, W. (2008) Acetylation is indispensable for p53 activation. *Cell. 133*, 612-26.
85. Tibbetts, R.S., Brumbaugh, K.M., Williams, J.M., Sarkaria, J.N., Cliby, W.A., Shieh, S.Y., Taya, Y., Prives, C., Abraham, R.T. (1999) A role for ATR in the DNA damage-induced phosphorylation of p53. *Genes Dev. 13*, 152-157.
86. Tokino, T. and Nakamura, Y. (2000)The role of p53-target genes in human cancer. *Crit Rev Oncol Hematol. 33*,1-6.
87. Tsukada, Y., Fang, J., Erdjument-Bromage, H., Warren, M.E., Borchers, C.H., Tempst, P., Zhang, Y. (2006) Histone demethylation by a family of JmjC domain-containing proteins. *Nature. 439*, 811-816.
88. Tzeng, T.T., Tsay, H.J., Chang, L., Hsu, C.L., Lai, T.H., Huang, F.L., Shiao, Y.J. (2013) Caspase 3 involves in neuroplasticity, microglial activation and neurogenesis in the mice hippocampus after intracerebral injection of kainic acid. *J Biomed Sci. 20*, 90.

89. Uemura, T., Shepherd, S., Ackerman, L., Jan, L.Y., Jan, Y.N. (1989) numb, a gene required in determination of cell fate during sensory organ formation in Drosophila embryos. *Cell. 58*, 349-360.
90. Vakoc, C.R., Sachdeva, M.M., Wang, H., Blobel, G.A. (2006) Profile of histone lysine methylation across transcribed mammalian chromatin. *Mol Cell Biol. 26*, 9185-9195.
91. Verdi, J.M., Bashirullah, A., Goldhawk, D.E., Kubu, C.J., Jamali, M., Meakin, S.O., Lipshitz, H.D. (1999) Distinct human NUMB isoforms regulate differentiation vs. proliferation in the neuronal lineage. *Proc Natl Acad Sci U S A. 96*, 10472-10476.
92. Węsierska-Gądek, J. and Schmidt, G. (2007) Transcriptional repression of anti-apoptotic proteins mediated by the tumor suppressor protein p53. *Cancer Ther/A>. 5*, 203-212.
93. Wu, Y., Tibrewal, N. and Birge, R.B. (2006) Phosphatidylserine recognition by phagocytes: a view to a kill. *Trends Cell Biol. 16*, 189-197.
94. Wu, Z., Zheng, S., Yu, Q. (2009) The E2F family and the role of E2F1 in apoptosis. *Int J Biochem Cell Biol. 41*, 2389-2397.
95. Xie, Q., Bai, Y., Wu, J., Sun, Y., Wang, Y., Zhang, Y., Mei, P., Yuan, Z. (2011) Methylation-mediated regulation of E2F1 in DNA damage-induced cell death. *J Recept Signal Transduct Res. 31*, 139-146.
96. Yan, B. (2010) Numb--from flies to humans. *Brain Dev. 32*, 293-8.
97. Yang, F., Teves, S.S., Kemp, C.J., Henikoff, S. (2014) Doxorubicin, DNA torsion, and chromatin dynamics. Biochim Biophys Acta. 1845, 84-89.
98. Yang, J., Xu, Z.P., Huang, Y., Hamrick, H.E., Duerksen-Hughes, P.J., Yu, Y.N. (2004) ATM and ATR: Sensing DNA damage. *World J Gastroenterol. 10*, 155-160.
99. Yogosawa, S., Miyauchi, Y., Honda, R., Tanaka, H., Yasuda, H. (2008) NUMB controls p53 tumour suppressor activity. *Nature. 451*, 76–80.
100. Yokoyama, A., Okuno, Y., Chikanishi, T., Hashiba, W., Sekine, H., Fujiki, R., Kato, S. (2010) KIAA1718 is a histone demethylase that erases repressive histone methyl marks. *Genes Cells. 15*, 867-73.
101. Yue, W.W., Hozjan, V., Ge, W., Loenarz, C., Cooper, C.D., Schofield, C.J., Kavanagh, K.L., Oppermann, U., McDonough, M.A. (2010) Crystal structure of the PHF8 Jumonji domain, an Nepsilon-methyl lysine demethylase. *FEBS Lett. 584*, 825-830.
102. Zhang, Y. and Reinberg, D. (2001) Transcription regulation by histone methylation: interplay between different covalent modifications of the core histone tails. *Genes Dev.15*, 2343-60.
103. Zhong, W., Jiang, M.M., Weinmaster, G., Jan, L.Y., Jan, Y.N. (1997) Differential expression of mammalian Numb, Numb-like and Notch1 suggests distinct roles during mouse cortical neurogenesis. *Development. 124*, 1887–1897.

Appendices

Appendix A. Raw PHF8 knockdown flow cytometry data of three biological replicates. The upper sets of histograms represent the apoptotic cells from samples treated with doxorubicin. The lower sets of histograms are the untreated samples. PHF8 knockdown cells are represented by the red line while control siRNA transfected cells are represented in blue. Western blot analysis demonstrates sufficient PHF8 knock down (bottom panel).

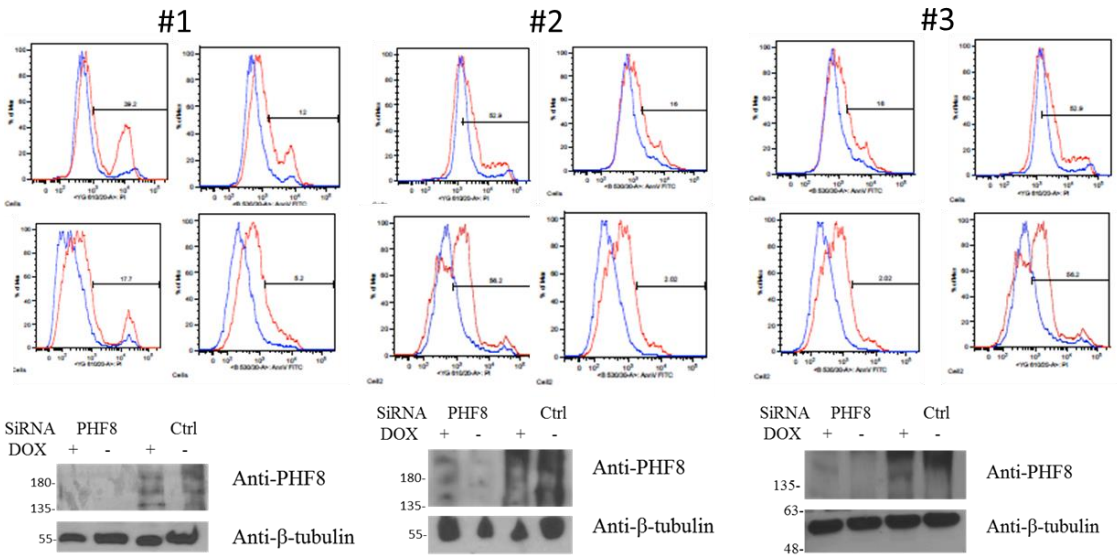

Appendix B: Raw PHF8 over expression flow cytometry data of three biological replicates. The upper sets of histograms represent the apoptotic cells from samples treated with doxorubicin. The lower sets of histograms are the untreated samples. PHF8 overexpressing cells are represented by the red line while pFLAG-CMV transfected cells are represented in blue. Western blot analysis demonstrates sufficient PHF8 over expression (bottom panel).

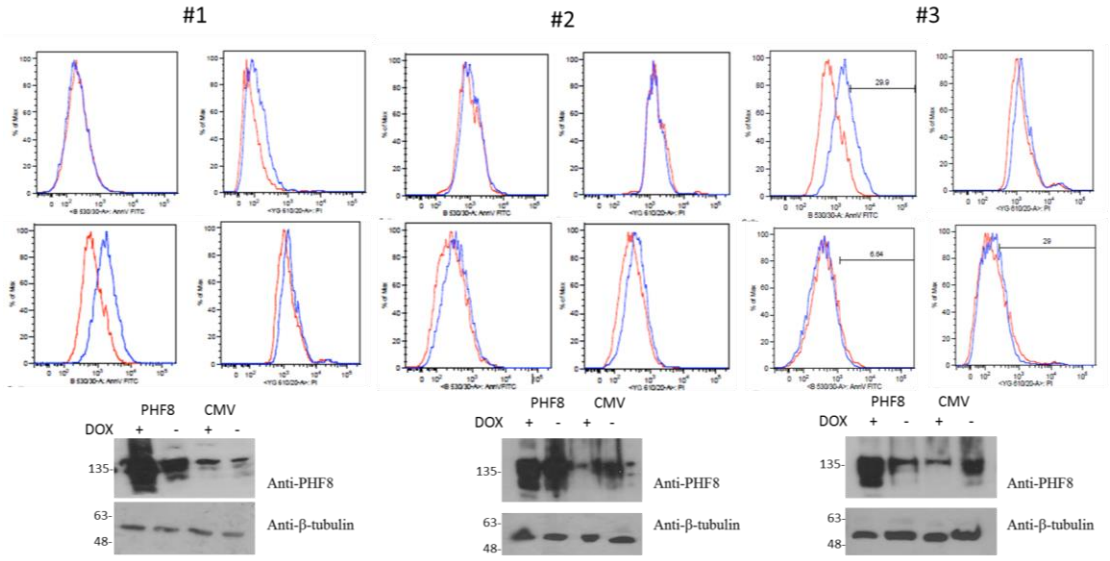

Curriculum Vitae

Name:	Kimberly Muranko
Post-secondary Education and Degrees:	University of Western Ontario London, Ontario, Canada 2007-2011 B.M.Sc.
Honours and Awards:	Dean's Honor List 2011 Western Graduate Research Scholarship 2012-2013
Related Work Experience	Teaching Assistant University of Western Ontario 2012-2013

Publications:

Dhami GK, Liu H, Galka M, Voss C, Wei R, Muranko K, Kaneko T, Cregan SP, Li L, Li SS.. (2013). Dynamic methylation of Numb by Set8 regulates its binding to p53 and apoptosis. Molecular Cell, 50(4):565-76.